

THE SECOND VERIFICATION OF THE ORIGINS OF ROTATION IN TORNADOES EXPERIMENT

VORTEX2

BY JOSHUA WURMAN, DAVID DOWELL, YVETTE RICHARDSON, PAUL MARKOWSKI, ERIK RASMUSSEN, DONALD BURGESS, LOUIS WICKER, AND HOWARD B. BLUESTEIN

VORTEX2 is the largest, most ambitious study focused on improving our understanding of tornadoes, including tornadogenesis, tornado structure, and improving forecasts.

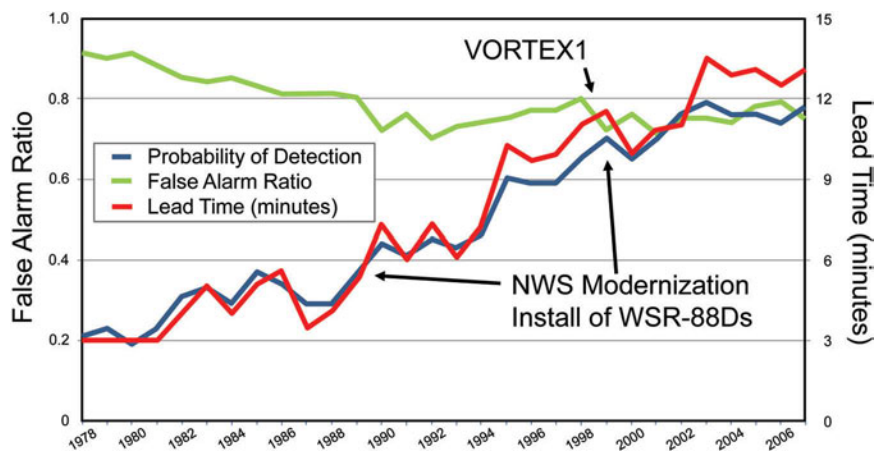


FIG. 1. History of lead times, probability of detection, and false-alarm rates for tornado warnings. Improvements in warning performance are related to introductions of new technology and forecasting methods.

Nearly all of the most intense tornadoes, those capable of causing the most widespread damage and largest number of fatalities, are spawned by supercell thunderstorms. Recently, computer models and observing technology used to study supercells have become more accessible and increasingly sophisticated, enabling detailed scientific exploration of supercells and tornadoes. Improvements to tornado forecasts and warnings in recent decades may be linked to improvements in observing technology and understanding of processes related to tornado formation (Fig. 1). Although these advances have led to an increase in knowledge and improvements to conceptual models of the processes governing tornadic storms, they also have illuminated gaps in our understanding of tornadogenesis and evolution, particularly those aspects of the problem that require contemporaneous knowledge of ►

the wind, thermodynamic, and precipitation fields in and around supercells.

These gaps in our knowledge, and improvements in observing capabilities, motivated the second Verification of the Origins of Rotation in Tornadoes Experiment (VORTEX2) as a successor to the original VORTEX (VORTEX1) and other smaller follow-on programs. Using the latest developments in quickly deployable observing technology, the primary objectives of VORTEX2 were to obtain simultaneous wind, precipitation (p), and thermodynamic data to i) better understand and document the processes underlying tornadogenesis, intensification, maintenance, and demise; ii) identify properties of the local environment that are influential in the tornado life cycle; iii) improve computer modeling and prediction of supercell thunderstorms and tornadoes; and iv) improve our understanding of the near-surface structure of tornadoes and the relationship between tornadic winds and damage.

The overarching goal of VORTEX2 was to improve the understanding of the processes thought essential to improving the accuracy, lead time, and false-alarm rates of tornado warnings. Delineating the subtle, poorly understood, and/or difficult-to-observe differences among nontornadic supercells, weakly tornadic supercells, and violently tornadic supercells would further this improvement. Additional objectives of VORTEX2, thought to be important for improving forecast skill, were to determine how storms interact with each other and with their local environment and how these interactions

affect tornado genesis, maintenance, and demise. Data collected by VORTEX2 also will be used for the development of storm-scale numerical weather prediction (NWP) systems. Finally, because many of the details concerning tornado structure are not well understood, such as the vertical distribution of winds and the intensity and variability of winds near the surface, VORTEX2 sought detailed documentation of tornado structure and its relationship to damage.

RECENT OBSERVATIONAL STUDIES OF SUPERCELLS AND TORNADOES.

Our knowledge of tornadoes and supercell storms progressed substantially during the latter portion of the previous century (e.g., Ludlam 1963; Lemon and Doswell 1979; Doswell and Burgess 1993; Davies-Jones et al. 2001; Markowski and Richardson 2009). However, until the mid-1990s, much of this understanding arose from theoretical, laboratory, and numerical models as well as from low-resolution observational studies. Major portions of the conceptual understanding of tornadogenesis were unverified by actual observations.

VORTEX1: 1994–95. A pivotal moment occurred in 1994–95, when VORTEX1 established a new experimental paradigm and pioneered a decade of targeted, mobile experiments that focused on tornadic storms and greatly enhanced our understanding of supercell thunderstorms (Rasmussen et al. 1994). Potentially tornadic storms were targeted by an array of instrumentation, including a quickly scanning mobile Doppler radar (Wurman et al. 1997; Wurman 2001, 2008), FM-CW and W-band radars (Bluestein et al. 1995, 1997), an array of instrumented vehicles (the mobile mesonet; Straka et al. 1996), several mobile balloon sounding systems (Rust et al. 1990), several mobile photogrammetric teams, deployable in situ instrumentation (Winn et al. 1999), and an aircraft fitted with a pseudo-dual-Doppler radar system (Wakimoto and Atkins 1996). This targetable array of cutting-edge instrumentation permitted the study of tornadoes and supercells with a degree of detail and breadth never before achieved. VORTEX1 established the viability of employing a large, fully adaptable array of land- and air-based instrumentation to sample short-lived, rare, and nonstationary phenomena such as tornadoes. Data, techniques, and knowledge from VORTEX1 were used by many researchers (e.g., Wakimoto and Atkins 1996; Wurman et al. 1996a,b, 1997; Dowell and Bluestein 1997, 2002a,b; Markowski et al. 1998a,b,c, 2002, 2003, 2008; Wakimoto et al. 1998; Wakimoto and

AFFILIATIONS: WURMAN—Center for Severe Weather Research, Boulder, Colorado; DOWELL—Earth System Research Laboratory, National Oceanic and Atmospheric Administration, Boulder, Colorado; RICHARDSON AND MARKOWSKI—The Pennsylvania State University, University Park, Pennsylvania; RASMUSSEN—Rasmussen Systems, Mesa, Colorado; BURGESS—Cooperative Institute for Mesoscale Meteorological Studies, University of Oklahoma, Norman, Oklahoma; WICKER—National Severe Storms Laboratory, National Oceanic and Atmospheric Administration, Norman, Oklahoma; BLUESTEIN—University of Oklahoma, Norman, Oklahoma

CORRESPONDING AUTHOR: Joshua Wurman, Center for Severe Weather Research, 1945 Vassar Circle, Boulder, CO 80305

E-mail: jwurman@cswr.org

The abstract for this article can be found in this issue, following the table of contents.

DOI:10.1175/BAMS-D-11-00010.1

In final form 15 February 2012

©2012 American Meteorological Society

Liu 1998; Trapp 1999; Rasmussen et al. 2000, 2006; Wurman and Gill 2000; Ziegler et al. 2001; Gilmore and Wicker 2002; Fierro et al. 2006; Richardson et al. 2007; Straka et al. 2007) to advance our knowledge of tornadic storms.

VORTEX1 resulted in a qualitative change in our understanding of tornadic storms. Observations revealed striking kinematic similarities between tornadic and nontornadic supercells at scales just larger than the tornado, suggesting that tornadogenesis is a perhaps fragile process that may depend on subtle, unobserved differences in morphologies and processes within supercells and their ambient environments. As such, it is now known that both tornadic and nontornadic supercell storms can contain strong low-level mesocyclones (Trapp 1999; Markowski et al. 2011). Though the importance of downdrafts in tornadogenesis was hypothesized before VORTEX1 (e.g., Ludlam 1963; Davies-Jones 1982a,b), VORTEX1 field observations and recent idealized simulations suggest that the thermodynamic properties of the downdraft may play an important role in modulating tornado formation and intensity (Markowski et al. 2002, 2003). Our awareness of the prevalence of mesoscale heterogeneities, such as those associated with outflow boundaries and anvil shadows in the supercell environment, has been heightened, leading to numerical simulations to study their effects on the evolution of convective storms (Atkins et al. 1999; Gilmore and Wicker 2002; Fierro et al. 2006; Richardson et al. 2007; Frame and Markowski 2010). Strong and violent tornadoes often were found to be associated with preexisting mesoscale boundaries (Markowski et al. 1998c).

Additionally, finescale observations of tornado structure and evolution were first obtained during VORTEX1. The first detailed three-dimensional maps of the winds in tornadoes were obtained by the prototype Doppler on Wheels (DOW) mobile radar. These three-dimensional maps of the core flow and surrounding regions with fine temporal and spatial resolution permitted the documentation of the horizontal (H) and vertical (V) distribution of intense winds and their evolution, central downdrafts, rapid changes in tornado structure, and the vertical and horizontal distribution of debris (Wurman et al. 1996a,b; Wurman and Gill 2000; Rasmussen and Straka 2007).

Post-VORTEX1 field projects. Building on the adaptive, targeted experimental design of VORTEX1, several smaller field programs focusing on tornadoes and supercell thunderstorms were undertaken

during the 1996–2008 period. Several programs, such as sub-VORTEX with rear-flank downdraft (RFD; (Markowski et al. 2002; Shabbott and Markowski 2006) and Analysis of the Near-Surface Wind and Environment along the Rear-Flank of Supercells (ANSWERS) concentrated on thermodynamic observations, primarily using mobile mesonet vehicles to study the properties of downdrafts and their relationship to tornadogenesis (e.g., Lee et al. 2004; Lee et al. 2011). Other field projects including the Radar Observation of Thunderstorms and Tornadoes Experiment (ROTATE; Wurman 1998, 1999, 2003, 2008), utilized mobile or quickly deployable high-resolution radars to study tornadogenesis and maintenance (Dowell et al. 2002; Bluestein et al. 2003a; Wurman et al. 2007b,c; Marquis et al. 2008; Wurman et al. 2010; Marquis et al. 2012); tornado structure (Wurman 2002; Bluestein et al. 2003b, 2004; Alexander and Wurman 2005; Lee and Wurman 2005; Bluestein et al. 2007a,b; Tanamachi et al. 2007; Kosiba et al. 2008; Kosiba and Wurman 2010); storm-scale processes coincident with tornadogenesis (Wurman et al. 2007c; Biggerstaff et al. 2008; Byko et al. 2009); the relationship between tornadic winds, debris, and damage (Burgess et al. 2002; Wurman and Alexander 2005; Dowell et al. 2005; Wurman et al. 2007a); and supercells that did not produce tornadoes (Beck et al. 2006; Frame et al. 2009; Markowski et al. 2011). ROTATE operated 12 of the 13 post-VORTEX2 years (1996–2001 and 2003–08) and utilized up to three DOWs, including a rapid-scan DOW (Wurman et al. 2008), mobile mesonet vehicles, and 12 instrumented in situ tornado pods. It collected single- and/or dual-Doppler data in approximately 140 different tornadoes and in many nontornadic supercells, allowing for the construction of a radar-based climatology of tornado characteristics and kinematics (Alexander and Wurman 2008; Alexander 2010).

MAJOR OUTSTANDING QUESTIONS IN TORNADO SCIENCE.

Although the aforementioned studies have continued to advance our understanding of tornadoes and supercell storms, the lack of contemporaneous thermodynamic data and high-resolution, radar-derived wind fields has limited the ability of these studies to fully diagnose the processes involved with tornadogenesis, evolution, and structure, because the development of low-level rotation is likely to depend on both the vorticity present in the environment as well as that developed baroclinically within the storm's cold pool. Evaluating the contributions of each of these requires knowledge of both the wind and thermodynamic

fields over multiple spatial scales and over temporal periods extending far enough before tornadogenesis that parcels participating in the genesis process can be traced back through the storm, revealing the source of rotation. Recently, several data assimilation techniques for convective-scale models have been utilized to retrieve the three-dimensional thermodynamic and hydrometeor fields from single-Doppler data (e.g., Dowell et al. 2004; Marquis et al. 2012) but, without observations to verify or refute model-generated output, the veracity of these computer-generated fields remains largely untested. Several key focus areas requiring additional study were identified.

Tornadogenesis. The most pressing problems in tornado science are centered on predicting the occurrence of significant tornadoes [i.e., tornadoes capable of inflicting damage corresponding to an enhanced Fujita (EF) scale rating of 2 or higher]. Identifying those storms that will produce significant tornadoes is critical because most fatalities and catastrophic damage are associated with the small fraction of tornadoes that exhibit the most intense wind speeds (a fraction that may be larger than previously thought; (Alexander and Wurman 2008; Alexander 2010) and the even smaller fraction that impacts densely populated areas (Brooks and Doswell 2001; Wurman et al.

2007a). However, this identification is complicated by the following observations:

- although most significant tornadoes are spawned from supercell thunderstorms, most supercell thunderstorms do not produce tornadoes and an even smaller fraction produce significant tornadoes (Trapp et al. 2005);
- if a tornado does occur, it only occurs during a small portion of the lifetime of the supercell thunderstorm; and
- most tornadic supercell thunderstorms, even when producing tornadoes, do not produce significant tornadoes (Verbout et al. 2006).

A brief review of our current knowledge of tornadogenesis is presented here. The reader is referred to Davies-Jones et al. (2001) and Markowski and Richardson (2009) for more detailed reviews. In the absence of preexisting environmental vertical vorticity, supercell thunderstorms acquire midlevel rotation through the tilting of environmental horizontal vorticity by an updraft and the subsequent stretching of this now vertical vorticity by the horizontal convergence associated with the updraft (Rotunno 1981; Lilly 1982; Davies-Jones 1984). Although the tilting of horizontal vorticity solely by an updraft can produce

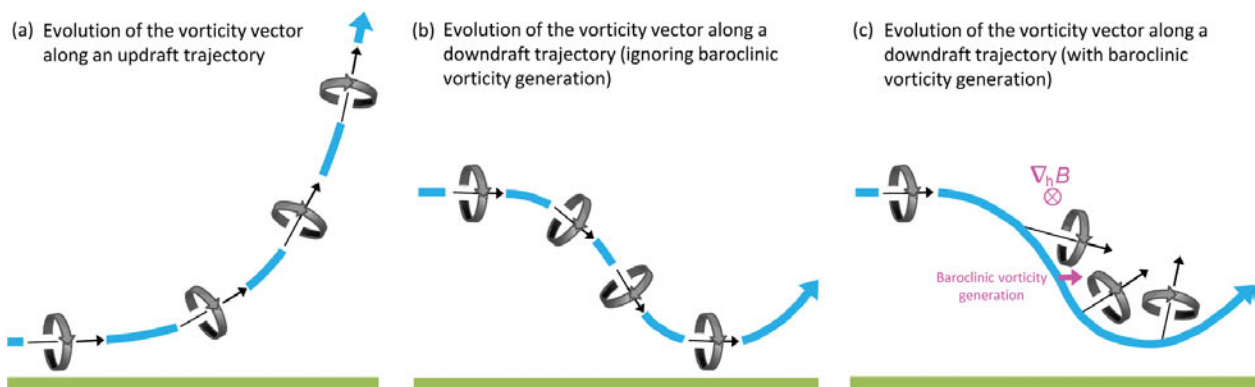


FIG. 2. Evolution of the vorticity vector (thin black arrows; the sense of rotation is indicated by the broad, curled black arrows) along trajectories (blue) in three situations. The upstream vorticity is streamwise in each case. (a) In the case of air rising through updraft, tilting of horizontal vorticity by the updraft alone cannot produce vertical vorticity at the surface because air is rising away from the surface as vertical vorticity is acquired. (b) In the case of air subsiding through a downdraft in which baroclinic vorticity generation is neglected, the horizontal vorticity is tilted downward during descent and returns to a horizontal orientation at the surface. (c) In the case of air subsiding through a downdraft in which horizontal vorticity is generated baroclinically by a horizontal buoyancy (B) gradient, such that warm air is into the page (the direction of vorticity generation is toward the right and indicated by the magenta arrow), the baroclinic vorticity generation introduces, in the words of Davies-Jones and Brooks (1993, p. 113), a “slippage between the descending fluid and vortex lines.” Subsequent tilting of the vorticity vector allows air parcels to reach the surface having cyclonic vorticity. Intense stretching can further amplify the vertical vorticity near the surface (such stretching probably requires that the downdraft parcels not be too negatively buoyant, lest they cannot ascend and be associated with large dw/dz). Here, (c) is adapted from Davies-Jones and Brooks (1993).

intense rotation at midlevels, no near-surface rotation is generated because vertical vorticity only develops as parcels rise away from the surface (Fig. 2). Therefore, downdrafts are critical in transporting and/or generating (through baroclinic effects and subsequent tilting) low-level vertical vorticity (e.g., Davies-Jones 1982a,b; Rotunno and Klemp 1985; Walko 1993; Davies-Jones and Brooks 1993; Straka et al. 2007). Indeed, dual-Doppler analyses (e.g., Brandes 1978; Dowell and Bluestein 1997; Wakimoto and Cai 2000; Dowell and Bluestein 2002a) and numerical simulations indicate that at least some air parcels pass through the RFD before entering the tornado (Wicker and Wilhelmson 1995).

Downdrafts have long been observed in the rear flanks of both tornadic and nontornadic supercells (e.g., Ludlam 1963; Fujita 1975; Burgess et al. 1977; Lemon and Doswell 1979). Surface observations of the RFD suggest that different combinations of microphysical and dynamical processes may be important in different supercells, at different locations within individual RFDs, and at different times in the same supercell (Markowski et al. 2002; Grzych et al. 2007; Hirth et al. 2008). Some tornadic supercells contain multiple rear-flank gust fronts (RFGFs; Wurman et al. 2007c; Marquis et al. 2008; Wurman et al. 2010; Marquis et al. 2012), suggesting that some forcing mechanisms may be transient and that RFD air reaching the ground nearly contemporaneously within the same supercell may reach the ground with substantially different thermodynamic properties (Finley and Lee 2004, 2008; Grzych et al. 2007). The relative importance of these processes in tornadogenesis is poorly understood.

Supercells and their environments. Understanding how the environments of supercell thunderstorms affect their propensity to cause tornadoes is critical to our ability to forecast tornadogenesis. Studies have shown that environmental variability and surface boundaries can affect storm structure and may instigate tornadogenesis (e.g., Maddox et al. 1980; Marwitz and Burgess 1994; Brooks et al. 1994, 1996; Weckwerth et al. 1996; Markowski et al. 1998c; Rasmussen et al. 2000; Richardson et al. 2007). Although many numerical studies have been conducted on isolated supercell thunderstorms (e.g., Rotunno and Klemp 1985), supercells in nature are rarely isolated and their environments are frequently complex (e.g., Ziegler et al. 2001). Supercells can develop from multiple smaller cells (Bluestein and Parker 1993), and rapid changes can occur after interaction with another cell (e.g., Lemon 1976; Lee et al. 2000; Bluestein and

Gaddy 2001; Hastings and Richardson 2010). Tornadogenesis may occur after storm mergers (Lee et al. 2000; Houston and Wilhelmson 2011; Dowell and Bluestein 2002a,b; Magsig and Dowell 2004). Wurman et al. (2007c) hypothesized that tornadoes resulting from cell mergers might tend to be weak and short lived. It is not clear which interactions promote tornadogenesis and which are detrimental.

Low-level winds in tornadoes. Computer, laboratory, and conceptual models of tornado vortices [for a more detailed review, see Davies-Jones et al. (2001)] remain largely unsubstantiated by reliable quantitative observations of actual tornadoes. In order to have confidence in conceptual models and theories developed from laboratory and numerical experiments, quantitative observations are needed in a variety of actual tornadoes having a variety of observed structures.

Although observational studies of the low-level and core-flow regions are challenging, observations by radar and in situ instruments occasionally have been obtained. The most frequent observations have been by mobile radars at close range to tornadoes (e.g., Wurman et al. 1996a,b, 1997; Wurman and Gill 2000; Bluestein and Pazmany 2000; Wurman 2002; Lee and Wurman 2005; Bluestein et al. 2004; Wurman and Alexander 2005; Alexander and Wurman 2005; Bluestein et al. 2007a; Tanamachi et al. 2007; Kosiba et al. 2008) and occasional in situ observations (Winn et al. 1999; Lee et al. 2004; Wurman and Samaras 2004; Wurman et al. 2007a). In a limited number of cases, some basic predictions of the conceptual and computational models have been confirmed, including the quasi-linear relationship between wind speed and distance to the axis of rotation in the core-flow region. Sub-tornado-scale vortices within large tornadoes also have been mapped (Wurman 2002; Alexander and Wurman 2005), as have the vertical distribution of wind speeds (Wurman et al. 1996a; Wurman and Gill 2000; Bluestein et al. 2004; Wurman and Samaras 2004; Alexander and Wurman 2005; Bluestein et al. 2007a; Wurman et al. 2007a), with suggestions of convergent inflow at the lowest levels (Alexander and Wurman 2005; Wurman et al. 2007a; Kosiba et al. 2008).

Model simulations with a wind engineering focus, such as those conducted by Fouts (2003), Sengupta et al. (2003), and Selvam and Millet (2003), have sought to modify traditional, straight-line wind engineering studies, including those based on wind tunnel experimentation. Preliminary results suggest that changing winds produce more damage than static wind conditions. McDonald (2001) and Marshall

(2002, 2004) have suggested that the wind speed–damage relationships implied in the original Fujita scale overestimate the peak winds in tornadoes. Based on comparisons of direct radar observations and observed damage, Wurman and Alexander (2005) proposed that changing wind speeds and directions and/or the integrated effect of wind-speed moments are correlated with damage just as well as peak-wind-gust Fujita-scale-type metrics. Except for this single case, there exists no extensive field validation of measured winds compared to a diverse range of damage. Consequently, until the actual nature of the tornado low-level wind threat can be better quantified, building codes cannot be intelligently designed to mitigate this threat.

Storm-scale NWP. During VORTEX2 field operations, the forecasting and field coordination team incorporated experimental real-time convection-allowing NWP models (Clark et al. 2011) into the process of selecting target regions and anticipating convective-storm evolution. Supporting the development of the next generation of high-resolution NWP systems (Stensrud et al. 2010; Xue et al. 2000), VORTEX2 NWP research is focusing on analysis and prediction of supercells, mesocyclones, and tornadoes; assessment of parameterization errors for storm-scale models; optimal use of observations; and analysis and prediction of the prestorm mesoscale environment. Unprecedented multisensor and multiscale observations obtained in the field are available for model initialization and forecast verification, enabling one to determine the optimal mix of observations, adaptive observing strategies, data assimilation methods, and forecast models needed for successful storm-scale NWP.

THE VORTEX2 FIELD EXPERIMENT.

Although VORTEX1 and other projects have increased substantially our knowledge of tornadogenesis, evolution, and structure, key questions remain and appear not to be fully addressable using only the observations provided by these efforts. Specifically, there is a need to observe supercell evolution prior to and during tornadogenesis as well as during the entire life cycle of the tornado. At minimum, these observations need to span periods of 1000–2000 s in order to capture key evolutionary processes. In addition, simultaneous radar observations must be obtained at multiple scales, including the storm scale, covering substantial portions of the supercell up to well above the melting layer; the mesocyclone scale, resolving the kilometer-scale flow surrounding the

tornado throughout the rear-flank region; and the tornado scale, resolving the tornadic circulation itself. Storm- and mesocyclone-scale radar observations should allow for dual-Doppler synthesis to reconstruct important kinematic fields (e.g., vorticity and divergence) within and around the storm. Critically, contemporaneous thermodynamic data are required in various regions of the storms, particularly in the inflow, across gust fronts, and within the rear- and forward-flank downdraft regions.

VORTEX2, managed by a steering committee comprising the authors of this report, was designed to address these questions. Documentation related to VORTEX2, including the scientific program overview (SPO), experimental design overview (EDO), and operations plan, as well as lists of principal investigators, instrumentation, and other information, can be found at the VORTEX2 website (www.vortex2.org). A field catalog is maintained by the National Center for Atmospheric Research (NCAR; at http://catalog.eol.ucar.edu/vortex2_2010 and http://catalog.eol.ucar.edu/vortex2_2009).

Project domain and nomadic plan. In order to maximize the number of tornadic supercells intercepted, VORTEX2 operations followed the ROTATE nomadic model and were conducted in a substantially larger area of the Great Plains than was done in VORTEX1, extending from the Dakotas to southwestern Texas and from Colorado/Wyoming to Iowa/Missouri, covering more than 1.2×10^6 km² (Fig. 3). Operations in urban areas, in hilly and/or forested terrain, and in areas with few roads were avoided when possible.

Data collection phase. Tornadoes are of short duration, and they occur relatively infrequently, irregularly, and in different geographical locations each year. Planning an experiment that targeted such a fickle phenomenon posed unique challenges. Ideally, one would conduct a many-year study and operate throughout the entire peak tornado season, which extends from March until July (Brooks and Doswell 2001) but, because of limitations of funding and staffing, it was impractical to do so. The ROTATE project, which intercepted approximately 140 tornadoes over 12 field seasons, provided a statistical basis for choosing the optimal field operation period and for estimating the level of success that could be reasonably anticipated by VORTEX2.

Operating over various spatial domains and time periods, sometimes shorter and smaller than planned for VORTEX2, ROTATE observed tornadoes on an average of 4.9 days per season and

significant tornadoes (F2/EF2 or greater), which were of the greatest interest to VORTEX2, on 1.3 days per season. Data were collected in zero significant tornadoes during 4 of the 12 seasons, yielding an F2+ “failure” rate of 33%. However, these failure seasons were uncorrelated and occurred during consecutive years only once, or 1 out of 11 possible seasons (9%). Thus, it was decided to spread the VORTEX2 field operations over two years, focusing on the most likely time for tornado occurrence in the Great Plains. Operations were planned for 10 May–15 June 2009 and 1 May–15 June 2010.

Observational strategies. One of the central and most ambitious goals of VORTEX2 was to obtain contemporaneous radar data at multiple scales (storm scale, mesocyclone scale, and tornado scale) in tandem with in situ thermodynamic and microphysical data collected by a combination of mobile mesonets, arrays of deployable weather stations (StickNet and pods), an unmanned aerial system (UAS), rawinsondes, and disdrometers. These integrated, multiplatform observations, at the surface and aloft, for long durations and at frequent intervals, were critical to testing many of the hypotheses related to tornadogenesis, evolution, and structure. VORTEX2 employed approximately 50 vehicles and was staffed by approximately 110 participants (Table 1), more than half of whom were students.

NESTING OF STORM-SCALE AND MESOCYCLONE-SCALE RADAR ARRAYS. The multiscale radar observations were accomplished by deploying nested groups of radars (Fig. 4). Storm-scale coverage was provided by two University of Oklahoma (OU) C-band (5.5 GHz) Shared Mobile Atmospheric Research and Teaching (SMART) radars (Biggerstaff et al. 2005) deployed approximately 20–30 km to the south of the forecast track of a supercell thunderstorm, with a baseline of ~35 km, resulting in a dual-Doppler surveillance area of ~1,500 km² and extending lengthwise for approximately 50 km along the storm’s path. Ideally, assuming a typical storm motion of 10 m s⁻¹, dual-Doppler observations through the entire depth of the storms could be obtained in this configuration for ~1.5 h. (Table 2)

An array of four X-band (9.4 GHz) radars from the Center for Severe Weather Research (CSWR) (DOW6 and DOW7), the National Severe Storms Laboratory (NSSL) (NOXP; Palmer et al. 2009), and the University of Massachusetts (UMASS) (UMASS XPOL; Kramar et al. 2005) ideally deployed in a line ~10 km to the south of the path of the hook of

the supercell, spaced 10–20 km apart, establishing an elongated region of fine-spatial-resolution dual-Doppler coverage along the path of the mesocyclone. As soon as the mesocyclone passed the rearmost X-band radar, that radar would move forward to the head of the X-band line, thereby ensuring continuous dual-Doppler coverage at the mesocyclone scale. The Mobile Weather Radar 2005 X-band Phased Array (MWR-05XP) (Bluestein et al. 2010a) would

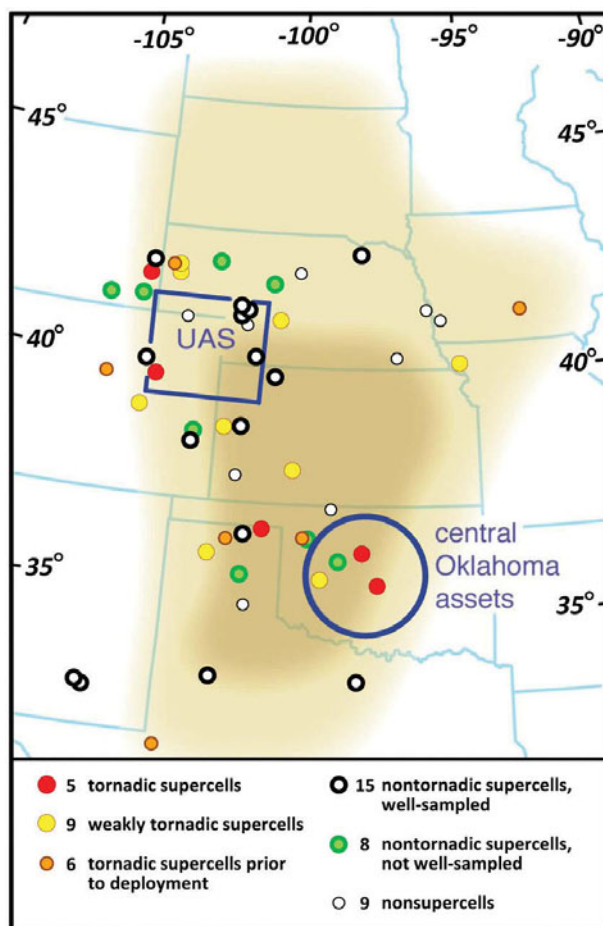


FIG. 3. The VORTEX2 operational domain. VORTEX2 operated in a nomadic fashion throughout a large portion of the high plains and surrounding area. Operations near certain fixed (Oklahoma) and restricted (UAS) assets were sometimes prioritized. Operations in the central portion of the domain (dark shade) were preferred because of superior terrain (fewer hills, trees, and urban areas) and road networks. Locations of VORTEX2 intercepts of various types of storms are indicated. During 2009–10, about 40 supercell thunderstorms were sampled, as summarized in the following: 5 tornadic supercells; 9 weakly tornadic supercells; 6 tornadic supercells prior to deployment; 15 nontornadic supercells well sampled; and 8 nontornadic supercells not well sampled. Nine nonsupercell storms are indicated.

TABLE I. List of major instruments and operating institutions.		
Instrument name	Operating institution	Description
SMART-RI	OU	C band (5 cm)
SMART-R2	OU	C band (5 cm), dual polarization
DOW6	CSWR	X band (3 cm), dual polarization, dual frequency, 18 m T, RH, Wind
DOW7	CSWR	X band (3 cm), dual polarization, dual frequency, 18 m T, RH, Wind
Rapid-scan DOW	CSWR	X band (3 cm), 6 simultaneous beam rapid scan, 14 m AGL, R, RH, Wind
NOXP	NSSL	X band (3 cm), dual polarization
UMASS XPOL	UMASS	X band (3 cm), dual polarization
TTUKa1	TTU	Ka band (1 cm)
TTUKa2	TTU	Ka band (1 cm)
UMASS-WV	UMASS	W band (3 mm)
MWR-05XP	NPS/CIRPAS	X band (3 cm), phased-array rapid scan
FC	NSSL	Communications and SASSI control center
Tornado pods (18 platforms)	CSWR (16), CU (2)	1-m wind, T, RH; hardened for in situ tornado measurements
StickNet (24 platforms)	TTU	2-m wind, T, RH; tripods
UAS	CU	Airborne T, RH
MGAUS	NSSL (2), NCAR (2), SUNY(1)	Mobile, van based, upsonde systems
Mobile mesonets	PSU/NSSL (6), CSWR (4)	3-m wind, T, RH, ρ ; vehicle mounted
Laser disdrometers	CU (2), UF (6), NSSL (1), NSSL/UI/NCAR (2)	Parsivel laser disdrometers
Photogrammetry	LSC, OU, NCAR	Cameras, some with integrated GPS navigation

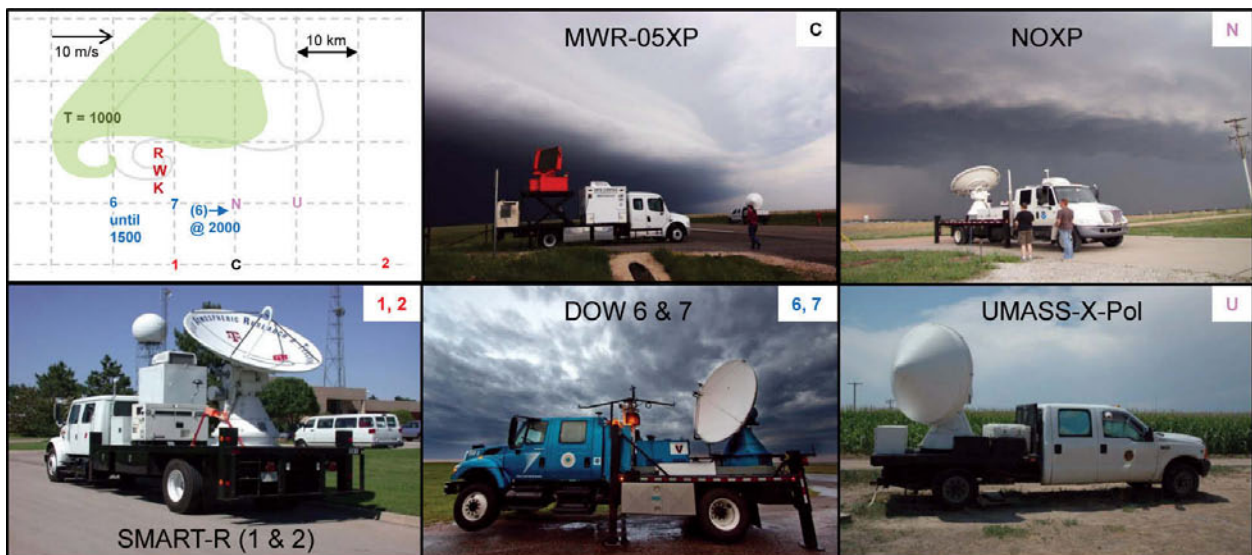


FIG. 4. VORTEX2 radars and deployment schematic: Storm- and mesocyclone-scale radars and a schematic of a typical deployment on a supercell. Storm-scale radars SMART-I (1), SMART-2 (2), and MWR-05XP (C) deploy well to the south of the storm, establishing long-duration, dual-Doppler coverage. Mesocyclone-scale radars DOW6 (6), DOW7 (7), NOXP (N), and UMASS XPOL (U) establish transient dual-Doppler baselines just to the south of the hook, leapfrogging in order to maintain continuous coverage. Tornado-scale radars (no photos shown) rapid-scan DOW (R), UMW (W), and TTUKa1, and TTUKa2 (K) deploy near to developing or existing tornadoes.

TABLE 2. Radar characteristics of VORTEX2 radars and lidar.

Radar name	Wavelength	Transmitter	Polarization	Volume time	Beam width, range resolution
SMART-R1	5 cm	mag 250 kW	H	180 s	1.5°, 63 m
SMART-R2	5 cm	mag 250 kW	Dual polarization	180 s	1.5°, 63 m
DOW6	2 × 3 cm	mag 2 × 250 kW	Dual polarization Dual frequency	120 s deep 60 s shallow	0.9°, 30–60 m
DOW7	2 × 3 cm	mag 2 × 250 kW	Dual polarization Dual frequency	120 s deep 60 s shallow	0.9°, 30–60 m
Rapid-scan DOW	3 cm	TWT 40 kW	H	7 s (rapid scan)	0.8°, 25–50 m
NOXP	3 cm	mag 250 kW	Dual polarization	120–180 s	1.0°, 75 m
UMASS XPOL	3 cm	mag 20 kW	Dual polarization	120–180 s	1.2°, 60–150 m
TTUKa1	1 cm	mag 10 kW	H		0.5°, 30 m
TTUKa2	1 cm	mag 10 kW	H		0.5°, 30 m
UMASS-W	3 mm	mag 1 kW	V		0.2°, 30–60 m
MWR-05XP	3 cm	TWT 15 kW	H	12 s (rapid scan)	2.0°, 75–150 m
TWO-LF	2 μm				

deploy to observe at the mesoscale and storm scale, providing deep volume updates at 7–14-s intervals.

A lidar system, the Truck-Mounted Wind Observing Lidar Facility (TWOLF), was attached to this platform (Bluestein et al. 2010b).

This was an idealized deployment strategy that was only approximately achieved in real-world conditions. However, on several occasions, nested storm-scale/mesocyclone-scale arrays were established successfully, such as on 9 June 2009 (Fig. 5).¹



FIG. 5. Snapshot of actual deployment of various radars. Storm and mesocyclone-scale radars are deployed in real-world road and terrain conditions in Kansas on 9 Jun 2009 on a marginally tornadic supercell to establish multiple-Doppler coverage.

SURFACE AND AIRBORNE IN SITU OBSERVATIONS INTEGRATED INSIDE DUAL-DOPPLER AREAS. Temperature (*t*), relative humidity (RH), wind, and pressure measurements at the surface and aloft are needed to characterize the thermodynamic and kinematic properties of the air in and around supercells. Several platforms were used to collect these data within the radar

¹ These idealized deployment strategies were rarely realized in practice, because of complications related to real road networks, storm motion/morphology, and other logistics. Radars would sometimes experience delays; have difficulty finding deployment sites unblocked by trees, terrain, or buildings; malfunction; or be unable to redeploy owing to intense intervening precipitation, traffic, poor road networks, or even low clearance overpasses. In general, an attempt was made to have the rearmost radars move to the front of the array so that multiple-Doppler radar coverage was maintained as continuously as possible.

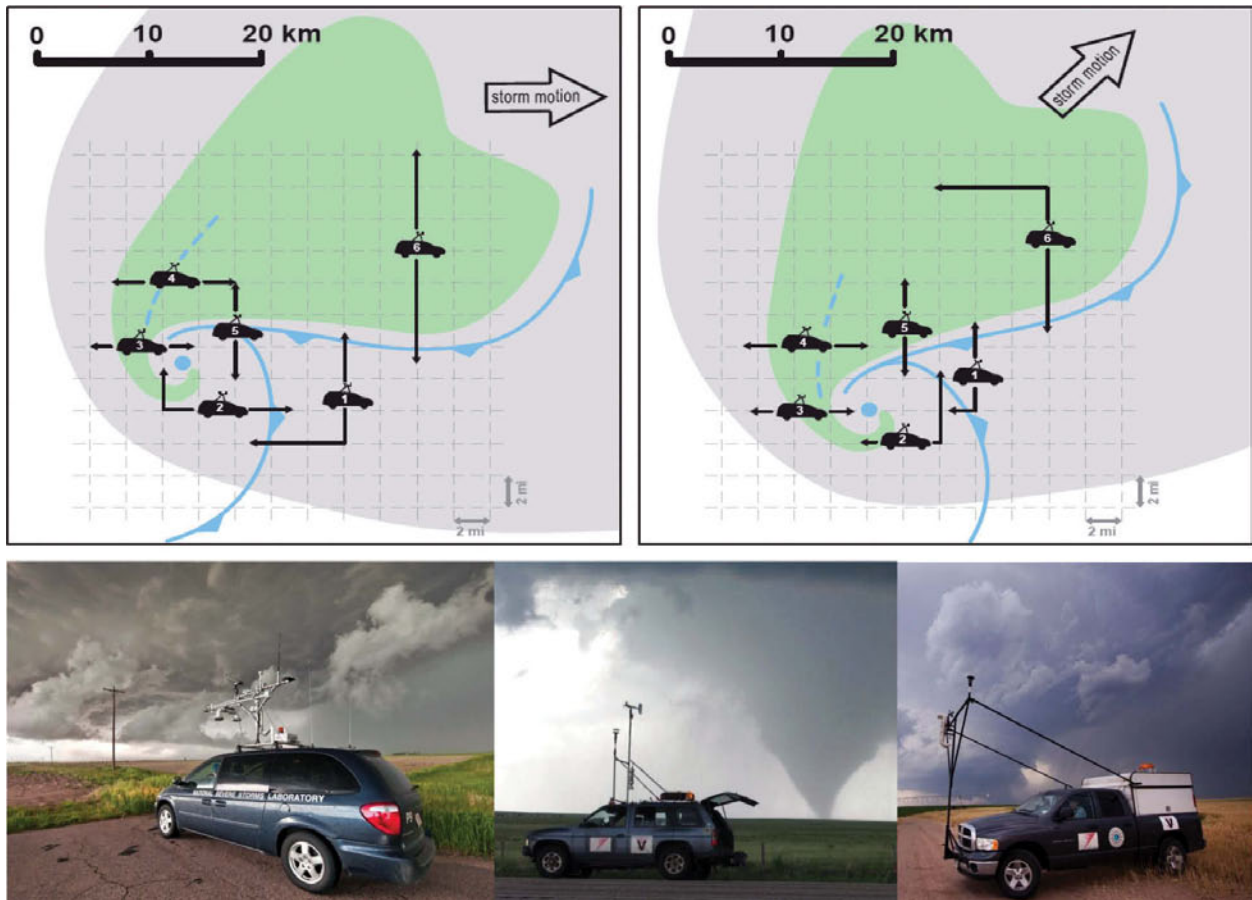


Fig. 6. Mobile mesonets used in VORTEX2 and schematic deployment routes through a slow-moving supercell.

coverage area. Mobile mesonets were tasked with conducting elaborate transects in various portions of the supercell, with a particular focus on the RFD, the forward-flank gust front (FFGF) and RFGF, and the primary inflow (Fig. 6). There were up to 11 mobile mesonet vehicles: 6 provided by NSSL [operated by The Pennsylvania State University (PSU) and NSSL], 1 provided by the Canadian Meteorological Service, and 4 combination pod/mesonet vehicles provided by CSWR.

The StickNet array, operated by Texas Tech University (TTU), consisted of 24 portable weather stations designed for deployment over large areas (Weiss and Schroeder 2008). Each StickNet probe consists of a tripod with weather instruments mounted at a height of approximately 1.5 m AGL (Fig. 7). The StickNet probes were deployed with a spacing of 1–5 km in lines ~20 km in length, ideally on several consecutive roads, in advance of the approaching supercell. StickNet deployments were designed to cover the span of a supercell, with an enhanced concentration near the forward-flank and rear-flank gust fronts.

During 2010, a UAS, operated by the University of Colorado (CU) and the University of Nebraska (UNL), provided information about the immediate storm environment aloft (Fig. 8). The UAS was launched near supercells and flew patterns outside the storms, but operations were limited by regulatory restrictions to airspace. Operations were permitted over only a small portion of the VORTEX2 domain (Fig. 3), so on many days when VORTEX2 intercepted supercells there were no UAS deployments.

TORNADO-SCALE OBSERVATIONS. Four (2009) and then six (2010) CSWR vehicles were equipped to carry a total of 16 pods (Fig. 9). Each pod contained an ultrasonic anemometer, a propeller anemometer, and a shielded temperature/relative humidity (T/RH) sensor at a height of 1 m (Wurman 2008). A data logger was housed in an armored waterproof box at the base. The entire package weighed approximately 50 kg and was designed to retain data in the event of high winds and/or debris damage. The pods were deployed in arrays to maximize the chance of achieving multiple transects through the

StickNet Deployment Strategy Slow-moving Storm (Default)

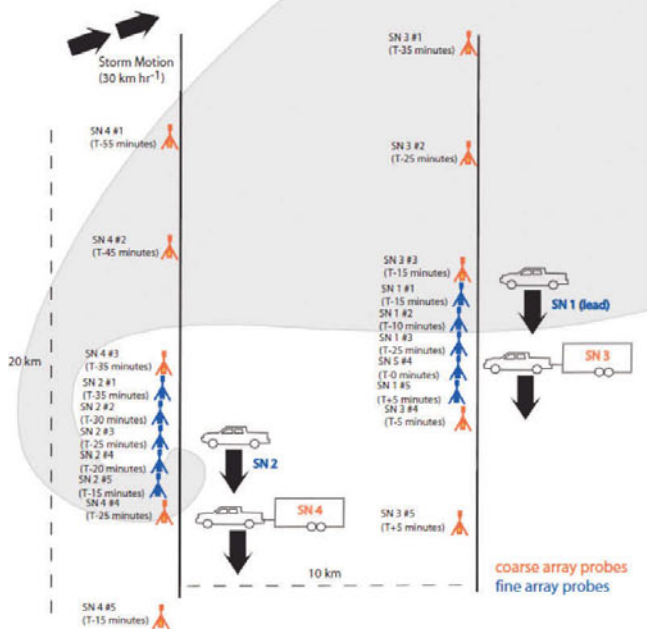


FIG. 7. A StickNet weather station and schematic deployment pattern.

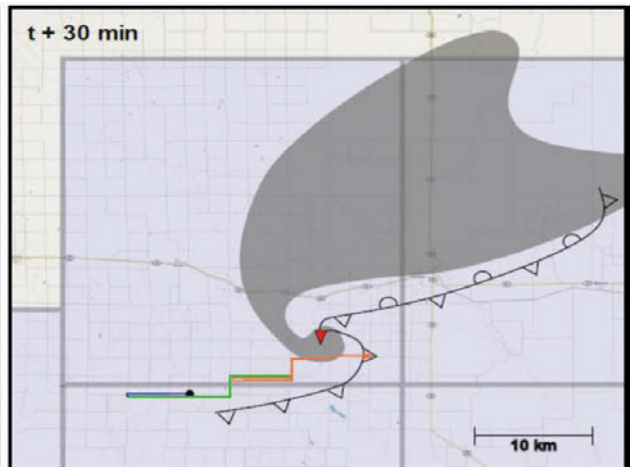


FIG. 8. UAS and schematic of flight pattern.

core and surrounding flow of a tornado. Pods also could supplement StickNet observations well away from the tornado, bringing the total possible number of deployable weather stations to 40.

The rapid-scan DOW (DOW5), the TTU Ka-band radars (TTUKa1 and TTUKa2) (Weiss et al. 2009), and UMASS W-band radar (UMW), having half-power beam widths of 0.8°, 0.5°, and 0.19°, respectively, provided data with very finescale

spatial resolution. These radars were deployed near to and south of the tornado track, scanning over the pod array, in order to provide 2D and 3D wind measurements from 15 to 1,000 m AGL (Fig. 10). The rapid-scan DOW provided fine temporal-spatial-scale volumetric updates at 7-s intervals. A pulsed Doppler lidar (TWOLF) on the MWR-05XP was used in 2010 for clear-air detection at ultra-high azimuthal resolution.

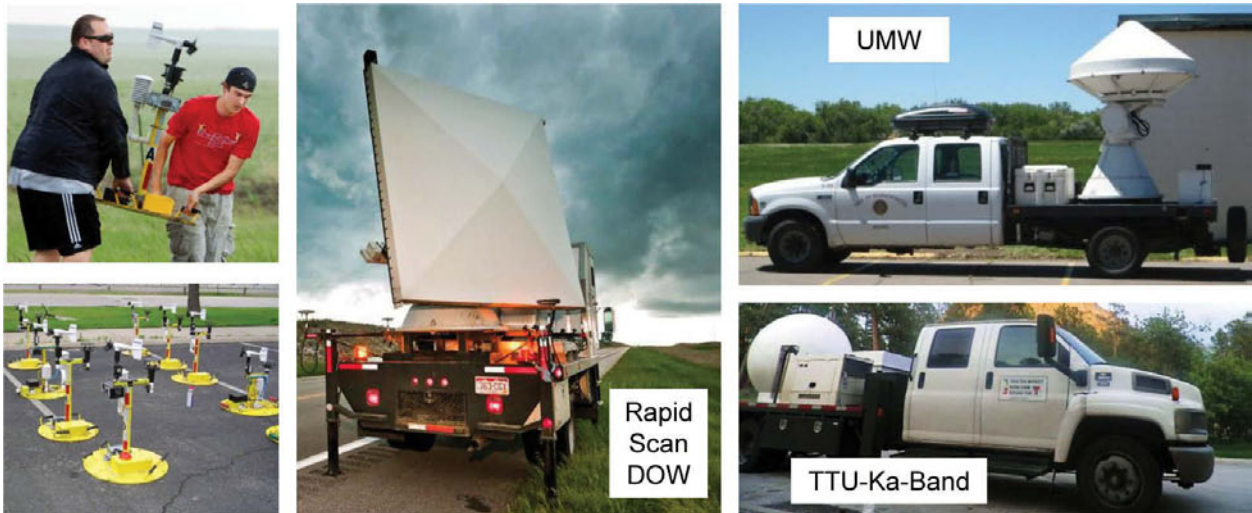


FIG. 9. A tornado pod and tornado-scale radars.

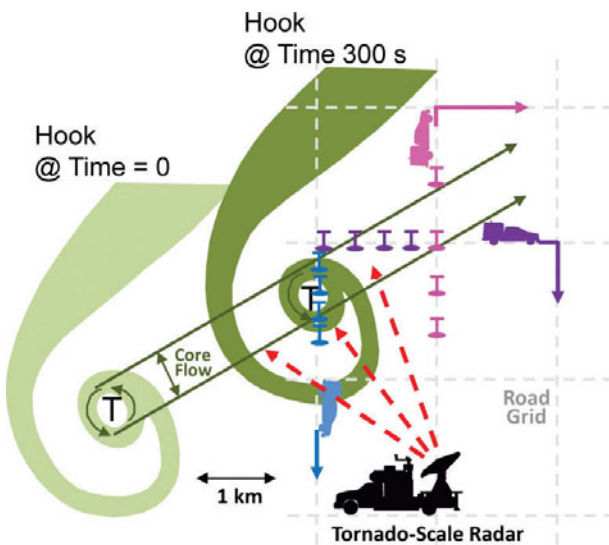


FIG. 10. Schematic diagram of deployment of tornado pod array with a tornado-scale radar scanning over the pods.

MICROPHYSICAL MEASUREMENTS USING RADARS AND DISDROMETERS. Testing of several hypotheses related to tornadogenesis requires knowledge of the microphysical properties of the precipitation in various portions of supercells. Several of the mobile radars had dual-polarization capability, including a SMART radar, UMASS XPOL, and NOXP. The DOW6 and DOW7 radars were upgraded for the 2010 season to dual-frequency, dual-polarization capability and could conduct quick-scanning dual-polarization measurements. All the dual-polarization radars had two missions because they were critical components of the nested dual-Doppler arrays described above. On each mission day, scanning was optimized either

for dual-polarization objectives (scanning through a deeper layer in the storm with slower updates) or for dual-Doppler objectives (shallower scanning with more rapid updates).

Several rapidly deployable disdrometers (Fig. 11), provided by the University of Colorado, the University of Florida (UF), the University of Illinois (UI), NCAR, and NSSL, were deployed in areas of the storm that had dual-polarization radar coverage in order to relate microphysical observations aloft to those at the surface.

STORM ENVIRONMENT MEASUREMENTS WITH SOUNDING SYSTEMS. In order to characterize the local environment in which supercells form and are maintained, Mobile GPS Advanced Upper-Air Sounding Systems (MGAUSSs), operated by NCAR, NSSL, and the State University of New York at Oswego (SUNY), launched instrumented balloons at frequent intervals near storms (Fig. 12). Sondes were launched prior to convective initiation in order to assist forecasting decisions and to capture changes in the local environment thought to be conducive to supercell formation. Once the supercell had formed, the environment surrounding the storm was sampled.

PHOTOGRAMMETRY AT TORNADO AND STORM SCALE. Photogrammetry teams from NCAR, Lyndon State College (LSC), and OU deployed at various locations near the storms (Fig. 12). Some of these teams were collocated with mesocyclone-scale radars, usually DOW6 and DOW7, or tornado-scale radars in order to conduct an integrated photographic-radar analysis of storm and tornado structure. These teams were also available for damage surveys. Other teams documented the evolution of various other portions of the supercell, such as the RFD.

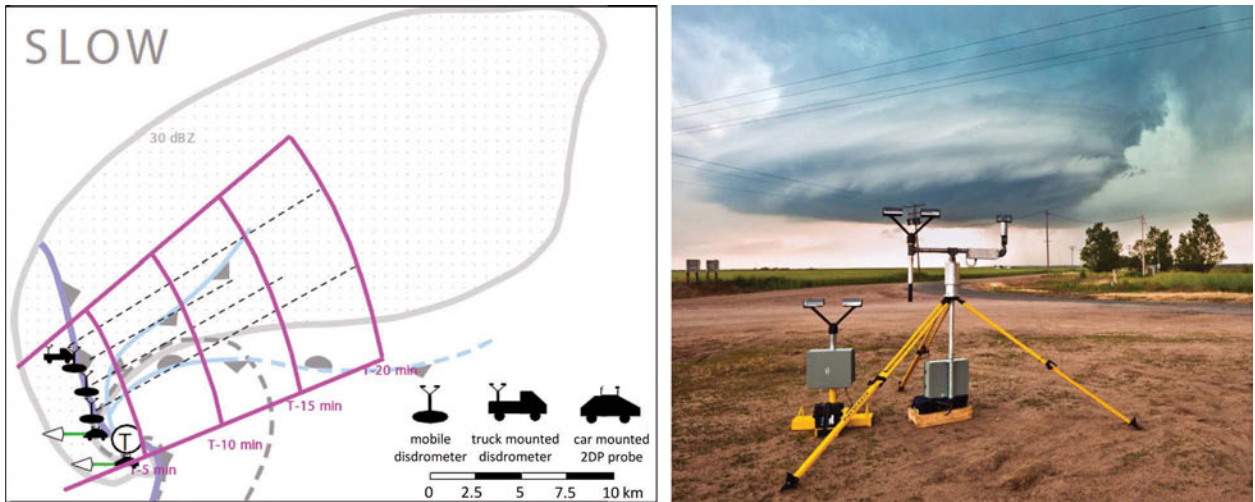


FIG. 11. Disdrometers and schematic deployment strategy.



FIG. 12. (left) Mobile balloon launching team. (middle) Photogrammetry equipment. (right) Schematic of deployment pattern.

Field logistics. The size and mobility of VORTEX2 posed unique challenges to achieving both safe and efficient field operations.

FORECASTING. Forecasting of target regions a day in advance of, on the morning of, and during the day of a mission was critical. Members of the VORTEX2 steering committee rotated through the morning forecast duties in 2009, whereas in 2010 members of a dedicated field forecast team led these discussions. During missions, forecasting was led by the field coordination team. VORTEX2 used imagery (ranging from environmental data to experimental numerical model guidance) obtained from the internet with mobile broadband systems, real-time Weather Surveillance Radar-1988 Doppler (WSR-88D) data, and real-time environmental and storm-scale data collected by VORTEX2 in the field (e.g., soundings, mobile-mesonet observations,

and radar data) to assess the rapidly evolving weather situations. Participants at the National Weather Center's Hazardous Weather Testbed facility assisted with forecasting, nowcasting, and facilitating communication with the National Weather Service, the Storm Prediction Center, and public safety officials with real-time information from the field.

COMMUNICATIONS AND COORDINATION. One of the most challenging aspects of VORTEX2 was the coordination of nearly 50 scientific vehicles. Deployment strategies were complex and fluid in rapidly changing weather scenarios. Supercell thunderstorms posed a risk to crew and vehicle safety, producing large hail; hazardous winds; frequent lightning; flash flooding; low visibility; hydroplaning hazards; and, of course, tornadoes with the attendant hazards associated with extremely high winds and airborne debris.

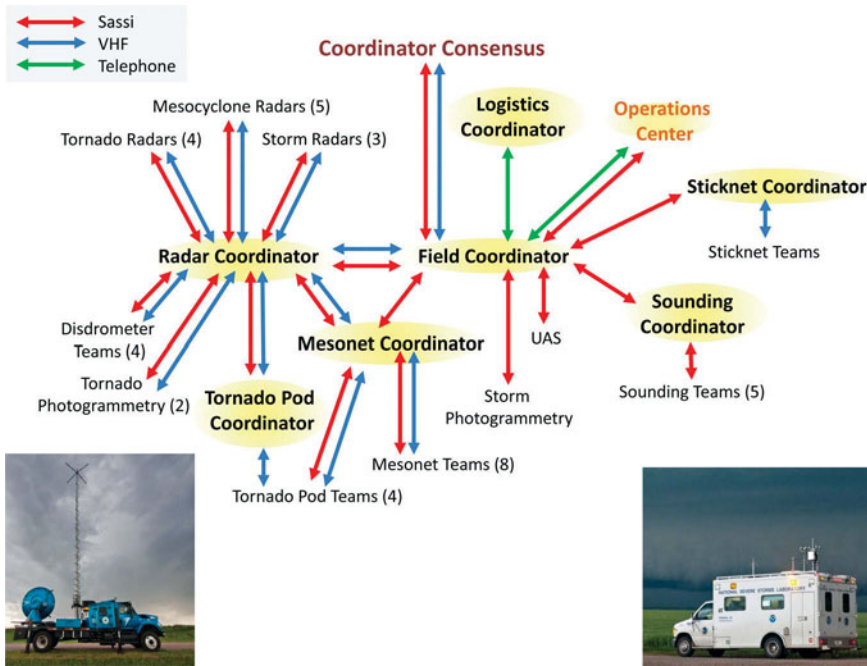


FIG. 13. Schematic of decentralized communications flow in VORTEX2. (right) FC managed SASSI, provided nowcasting and coordination for the VORTEX2 fleet, and provided communications with nonfield forecasters. (left) DOWs and other vehicles with masts could communicate and relay messages using VHF over long ranges.

Based on experiences from VORTEX1, ROTATE, sub-VORTEX-RFD, and other tornado studies, it was decided that decentralized coordination was critical because of the number and variety of vehicles, platforms, and missions. Thus, control of deployments was split among several coordinators: mobile mesonet, radar, field, UAS, balloon, etc. Overall targeting, forecasting, and logistical decisions were made through a consensus of these coordinators (Fig. 13). Initial mission and targeting decisions were made at morning meetings by consensus of the principal investigators, with a mission scientist (member of the VORTEX2 steering committee, according to a predetermined schedule) leading mission discussions and breaking ties, when needed.

To facilitate this decentralized control model, a high level of situational awareness among all the participants was needed. The Situational Awareness for Severe Storm Intercepts software (SASSI) was designed with this in mind, providing real-time vehicle tracking, weather display, and chat capabilities through cellular internet (Fig. 14). Participants and coordinators could communicate via chat with their team leaders and others. Coordinators could annotate maps to provide awareness of the forecast location of the mesocyclone, future multiple-Doppler lobes, and hazards such as washed out roads. SASSI

was controlled through a field coordination vehicle (FC), which provided nowcasting and strategic guidance.

Several teams operated very high-frequency (VHF) radios, some with power up to 200 W. Several platforms had pneumatic masts that could be raised (e.g., DOWs to 18 m AGL, the FC and a SMART radar to 13 m AGL) to achieve VHF ranges up to a few tens of kilometers. Intra-team communication among several of the radars, mobile mesonets, StickNet, and tornado pod teams was often conducted via VHF radio, particularly when an internet connection was not possible.

LODGING, FOOD, AND FUEL.

VORTEX2 had unique logistical challenges due to its fully nomadic nature, requiring lodging (~100 hotel rooms) for up to 160 participants and observers in different small cities every evening, with little notice. Each afternoon, a consensus decision was made concerning the overnight location for VORTEX2, even though the current day's mission often was far from complete. At times, fueling of over 50 vehicles and obtaining food and restroom services could overwhelm local facilities. We know of no precedent in any science project for billeting a group this large in different locations, on such repeatedly short notice.

PRELIMINARY RESULTS AND SUMMARY.

During the 2009 and 2010 field phases of VORTEX2, data were collected in about 40 supercells, about 14 of which produced tornadoes observed by at least some VORTEX2 instruments (Fig. 3). The year 2009 was very challenging for studying tornadic supercells. May 2009 was particularly quiescent and, consequently, many objectives of the VORTEX2 project were not achieved during this period. However, weather conditions became more propitious for scientific study in June 2009. In particular, a long-lived, strong tornado, which occurred in Wyoming on 5 June 2009, became the best-sampled tornadic supercell to date. Several other days in 2009, including 7, 9, and 11 June, yielded

data in nontornadic and weakly tornadic supercell thunderstorms. During 2010, data were obtained in over a dozen tornadic supercells. Particular events of interest include 10, 12, 19, and 25 May and 7 and 13 June. With the exception of 10 May 2010, most of these tornadoes were weak and/or short lived. A summary of the most interesting cases as identified by VORTEX2 PIs is provided in Table 3.

The integration of diverse datasets into coherent analyses is a complex process. In nearly all of the cases, combined multiple-Doppler and thermodynamic analysis are being conducted through collaborations among multiple groups. In addition to the listed cases, more specialized analyses, often focusing on data from unique or experimental instruments (i.e., TWOLF/MWR-05XP data and photogrammetry) also are being conducted. Analyses of these cases are ongoing and the final results will be published elsewhere. Some very preliminary results were presented at the American Meteorological Society's Severe Local Storms Conference in Denver, Colorado,

in October 2010 and at the Radar Meteorology Conference in Pittsburgh in 2011. An unofficial count revealed 46 individual presentations at the Denver meeting and 21 presentations at the Pittsburgh meeting that focused on or discussed preliminary results from VORTEX2.

Although final analyses are not complete, some preliminary examples of work in progress on one of the more comprehensive datasets are presented here, to illustrate the diversity of the observations and the potential for integration of different datasets to better understand these storms. On 5 June 2009, VORTEX2 observed the complete life cycle of a long-lived and strong tornado. Multiple radars, mobile mesonets, pods, disdrometers, StickNet, and photogrammetry teams were deployed during all or part of the tornado's lifetime. A long-duration dual-Doppler and mobile mesonet deployment was achieved (Fig. 14). At one time, at least six different radars were observing the storm (Fig. 15). Multiple-Doppler, mobile mesonet, and other data were collected from well before the

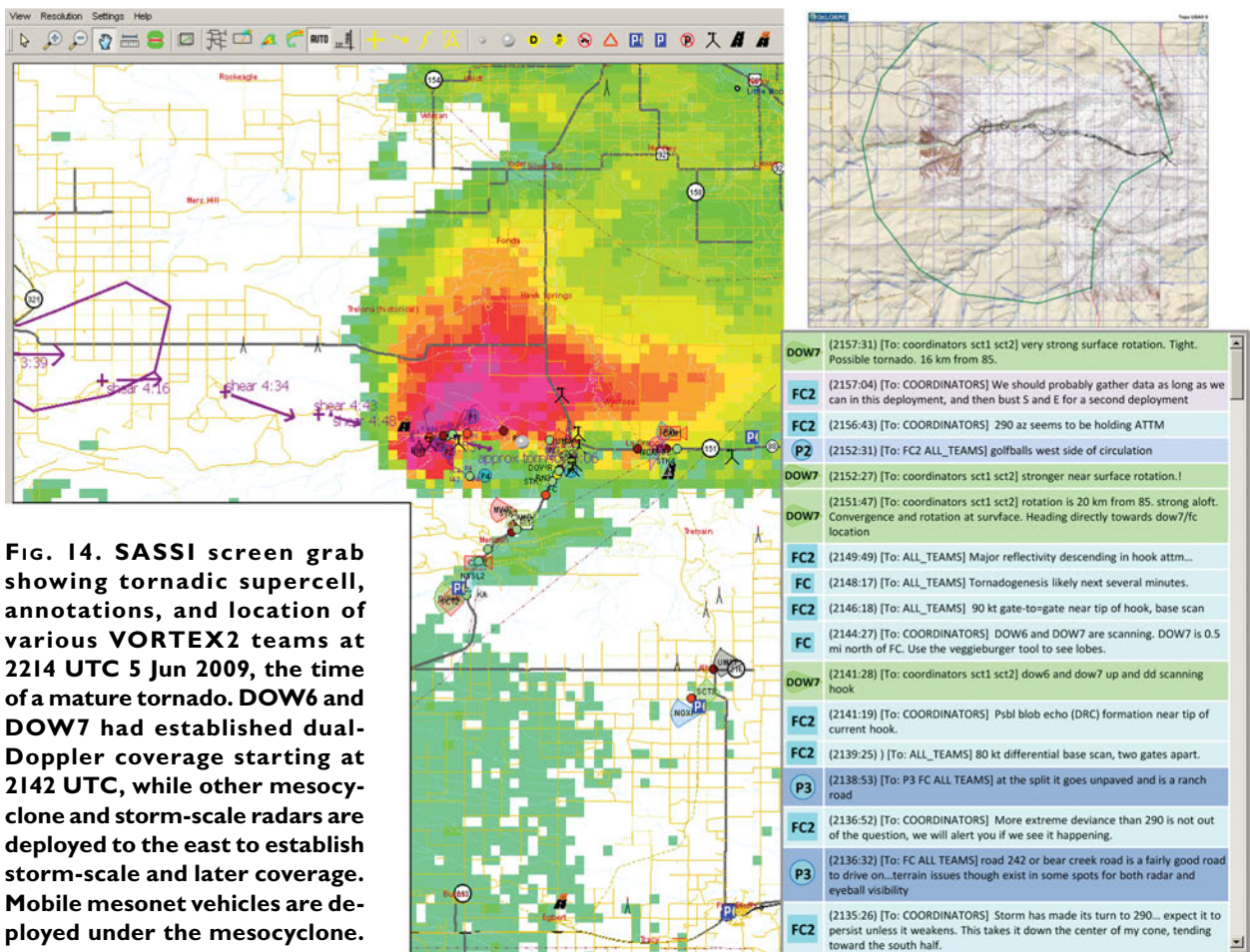


TABLE 3. High-priority analysis days from 2009 and 2010.

VORTEX2 cases—2009	Location	Description
15 May	Northwest OK	Squall line, mesovortices
5 Jun	Goshen County, WY	Tornadic and nontornadic supercells
7 Jun	Oregon to Maysville, MO	Weakly tornadic supercell
9 Jun	Ford to Greensburg, KS	Nontornadic supercell
11 Jun	La Junta to Lamar, CO	Nontornadic supercell pair
VORTEX2 cases—2010	Location	Description
6 May	Oberlin, KS	Elevated supercell
10 May	East-central OK	Tornado outbreak
12 May	Near Weatherford, OK	Weakly tornadic supercell
15 May	Near Artesia, NM	High-based storm
18 May	Dumas to Stinnett, TX	Tornado; classic → HP supercell
19 May	Near Kingfisher, OK	Weakly tornadic storm
24 May	Ogallala to Gothenburg, NE	Supercells, squall line, QLCS tornado
25 May	Tribune, KS	Landspouts and supercell tornadoes
26 May	Prospect Valley, CO	High-based nontornadic supercell
6 Jun	Grant and Ogallala, NE	Two nontornadic supercells
7 Jun	Mitchell and Scottsbluff, NE	Two tornadic supercells
10 Jun	Hoyt to Last Chance, CO	Nontornadic supercell, tornadic supercell
11 Jun	Limon to Bovina, CO	Weakly tornadic supercell
13 Jun	Perryton to Booker, TX, to Laverne, OK	Tornadic supercell
14 Jun	Wilson to Tahoka, TX	Supercell with gustnadoes, flooding

tornado formed through demise, revealing the kinematic and thermodynamic structures associated with multiple gust fronts, a descending reflectivity core (DRC), and the origins of air parcels entering the low-level mesocyclone and tornado.

Well prior to tornadogenesis, there were two distinct regions of significant cyclonic rotation: one region extended to low levels and was associated with vortex lines that arched upward out of the outflow (the orientation of these vortex lines strongly suggested they originated from baroclinic vorticity generation), and the other was associated with the midlevel mesocyclone, from which vortex lines extended into the warm sector to the south-southwest. The intensification of low-level rotation was preceded by the formation of a DRC, similar to others that have been documented in some supercells recently (Rasmussen et al. 2006; Kennedy et al. 2007a,b; Byko et al. 2009; Markowski et al. 2012a,b) (Fig. 16). During tornadogenesis, the rear-flank downdraft strengthened and a secondary rear-flank gust front similar to those recently documented in other tornadic supercells (Wurman et al. 2007a;

Marquis et al. 2008, 2012) formed. Orientation of the vortex lines/arches continued to suggest that the low-level circulation was baroclinically generated. Although the tornadic circulation primarily comprised parcels originating in the forward flank of the storm, not the rear flank, variation in secondary rear-flank downdraft strength was associated with increased convergence and tilting of horizontal vorticity near the tornadic circulation, tornadogenesis, and intensity changes in the nascent tornado (Kosiba et al. 2012, manuscript submitted to *Mon. Wea. Rev.*) (Fig. 17). Combined photogrammetric and radar analyses of the mature tornado indicate that the strongest winds near the surface were outside the visible condensation funnel and that there were separate maxima in the rotational wind, one near the surface and the other near the cloud base (Wakimoto et al. 2011; Atkins et al. 2012) (Fig. 18).

VORTEX2 is poised to address many important questions relating to tornadogenesis and tornado structure. It is also likely that analysis of the rich suite of new observations obtained by VORTEX2 will result in new, unanticipated questions. For example, an unexpected

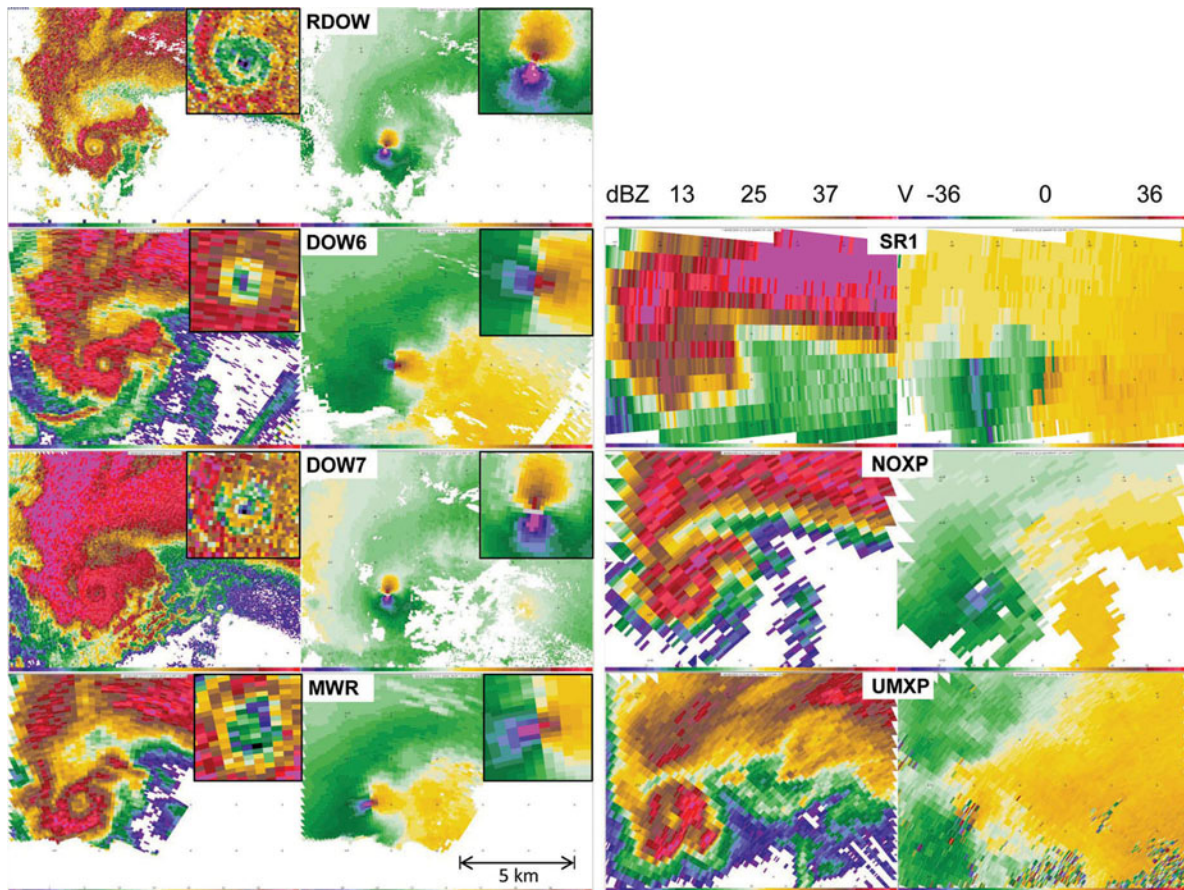


FIG. 15. Doppler velocity and reflectivity images of the 5 Jun 2009 Goshen County, Wyoming, tornadic supercell observed by seven VORTEX2 radars at approximately 2216 UTC. Viewing angles, native radar resolution, wavelength, and range to the tornado all affect the appearance of the supercell, hook echo, and tornadic region. RDOW: Rapid-Scan DOW, SRI: SMART-Radar 1, UMXP: UMASS XPol.

and as yet unexplained phenomena, a thin low-reflectivity ribbon (LRR) completely bisecting the forward and rear flanks of some supercells, was observed for the first time during VORTEX2. One LRR (5 June 2009) was characterized by deep (up to 25 dBZ) reflectivity deficit and very narrow (~600 m) width, and it extended through the full depth of a supercell, effectively bisecting the high-reflectivity regions of the forward flank and rear flank near the time of tornadogenesis. It was shown that air parcels

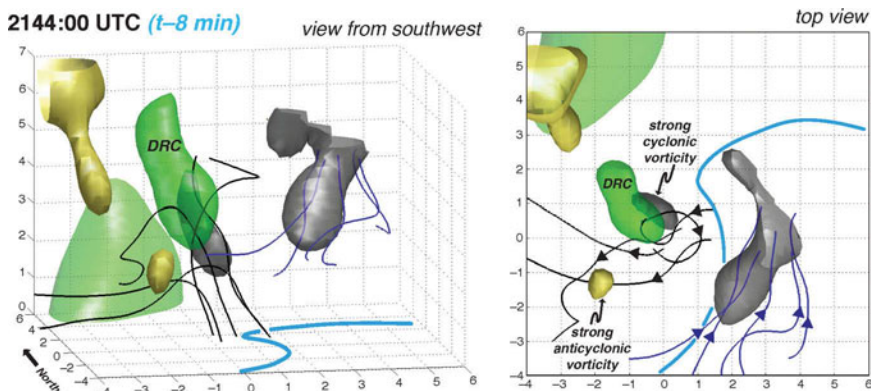


FIG. 16. View from the southwest and from above of the 55-dBZ DOW7 reflectivity isosurface (green) and vertical vorticity isosurfaces of 0.02 (gray), and -0.01 s^{-1} (yellow) at 2144 UTC 5 Jun 2009 (8 min prior to tornadogenesis). The gust front is indicated with a heavy cyan line. Vortex lines that pass through the midlevel mesocyclone are blue; these originate in the warm sector. Vortex lines that pass through the low-level mesocyclone are black and arch upward out of the outflow behind the gust front. In the view from above, the direction of the vorticity vector is indicated by the arrowheads. Axis labels are in kilometers (adapted from Markowski et al. 2012a).

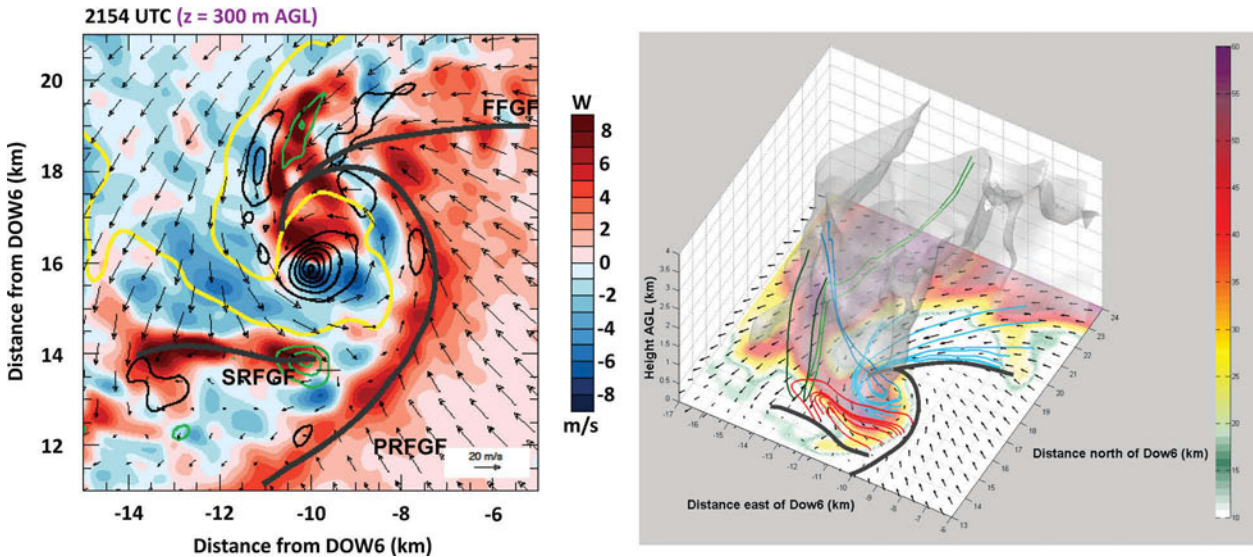


FIG. 17. (left) DOW6–DOW7 dual-Doppler winds at 300-m AGL during the tornadogenesis period. The yellow contour depicts the 30-dBZ DOW7 reflectivity isopleth, vectors represent the horizontal winds, shading depicts the vertical winds, black contours depict vertical vorticity > 0 , and green contours depict vertical vorticity < 0 and are contoured every 0.02 s^{-1} . The primary RFGF (PRFGF), secondary RFGF (SRFGF), and FFGF are delineated by solid gray lines. Evolution of the SRFGF was associated with changes in convergence and tilting of horizontal vorticity and modulations in nascent tornado intensity. (right) Air parcel trajectories enter the tornadic circulation from the forward flank (cyan) and rise (dark cyan). Parcels descending in the RFD (green) rise along the PRFGF (dark green). Vortex arches (red) suggest baroclinic generation of vorticity. Near-surface reflectivity is shaded in color and the 40-dBZ 3D isosurface is gray (adapted from Kosiba et al. 2012).

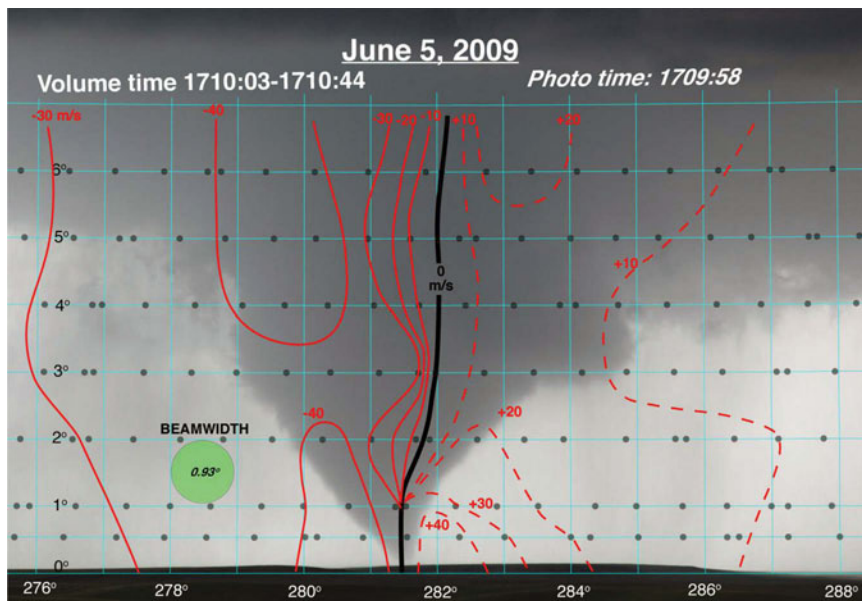


FIG. 18. Photogrammetric analysis of the 5 Jun 2009 tornado at 2210 UTC. Doppler winds (red contours) are overlaid over the visible image. Peak Doppler velocities are outside the visible condensation funnel at this time (adapted from Wakimoto et al. 2011).

entering a developing tornado passed near but not through the LRR (Kosiba et al. 2012, manuscript submitted to *Mon. Wea. Rev.*). Another LRR (13 June 2010), observed by multiple dual-polarization radars near

tornadic and nontornadic cases are expected to increase our understanding of the subtle differences between them, contributing to the goal of more accurate watches and warnings.

the time of tornadogenesis, exhibited a similar morphology and low differential reflectivity, suggestive of small rain droplets (Fig. 19). The role of these LRRs, if any, in tornadogenesis remains unclear and may inspire post-VORTEX2 study.

The field portion of the VORTEX2 project has concluded and analysis of the data is underway. The field phase resulted in unprecedentedly diverse data collection in several dozen tornadic and nontornadic supercell thunderstorms, as well as quasi-linear convective systems (QLCSs) (Bryan and Parker 2010) and other phenomena. Comparisons between the

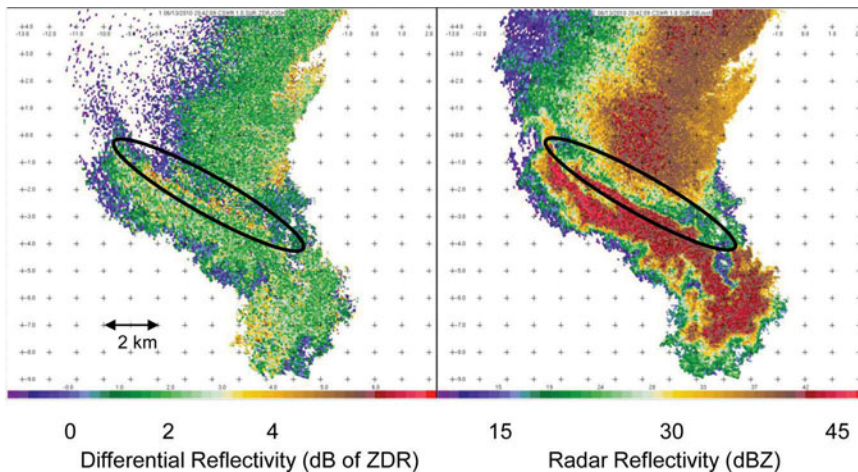


FIG. 19. LRR visible in (left) differential reflectivity and (right) radar reflectivity as observed by the DOW7 radar during VORTEX2 on 13 Jun 2010. A narrow region of substantially reduced reflectivity and low differential reflectivity, suggestive of small rain drops, completely separates the high-reflectivity forward and rear flanks of the storm.

ACKNOWLEDGMENTS. VORTEX2 was a collaborative effort among over two dozen principal investigators, engineers, technicians, and administrators at over a dozen different institutions, including over 80 undergraduate and graduate students. The National Science Foundation and the National Oceanic and Atmospheric Administration provided the primary financial support for VORTEX2. Preparation of this manuscript and VORTEX2 logistics were supported by NSF Grants ATM-0724318 and ATM-0801041. The Doppler On Wheels are supported through NSF ATM-0734001.

REFERENCES

Alexander, C. R., 2010: A mobile radar based climatology of supercell tornado structures and dynamics. Ph.D. dissertation, University of Oklahoma, 251 pp.

—, and J. Wurman, 2005: The 30 May 1998 Spencer, South Dakota, storm. Part I: The evolution and environment of the tornadoes. *Mon. Wea. Rev.*, **133**, 72–96.

—, and —, 2008: Updated mobile radar climatology of supercell tornado structures and dynamics. Preprints, *24th Conf. on Severe Local Storms*, Savannah, GA, Amer. Meteor. Soc., 19.4. [Available online at <http://ams.confex.com/ams/pdfpapers/141821.pdf>.]

Atkins, N. T., M. L. Weisman, and L. J. Wicker, 1999: The influence of preexisting boundaries on supercell evolution. *Mon. Wea. Rev.*, **127**, 2910–2927.

—, A. McGee, R. Ducharme, R. M. Wakimoto, and J. Wurman, 2012: The LaGrange tornado during VORTEX2. Part II: Photogrammetric analysis of the

tornado combined with dual-Doppler radar data. *Mon. Wea. Rev.*, in press.

Beck, J. R., J. L. Schroeder, and J. M. Wurman, 2006: High-resolution, dual-Doppler analyses of the 29 May 2001 Kress, Texas, cyclic supercell. *Mon. Wea. Rev.*, **134**, 3125–3148.

Biggerstaff, M. I., and Coauthors, 2005: The Shared Mobile Atmospheric Research and Teaching radar: A collaboration to enhance research and teaching. *Bull. Amer. Meteor. Soc.*, **86**, 1263–1274.

—, D. W. Burgess, G. D. Carrie, E. R. Mansell, L. J. Wicker, and C. L. Ziegler, 2008: Storm-scale sampling strategies for the mobile C-band Doppler radars during VORTEX2. Preprints, *24th Conf. on Severe Local Storms*, Savannah, GA, Amer. Meteor. Soc., 5.2. [Available online at https://ams.confex.com/ams/24SLS/techprogram/paper_141892.htm.]

Bluestein, H. B., and S. S. Parker, 1993: Modes of isolated, severe convective storm formation along the dryline. *Mon. Wea. Rev.*, **121**, 1354–1372.

—, and A. L. Pazmany, 2000: Observations of tornadoes and other convective phenomena with a mobile, 3-mm wavelength, Doppler radar: The spring 1999 field experiment. *Bull. Amer. Meteor. Soc.*, **81**, 2939–2351.

—, and S. G. Gaddy, 2001: Airborne pseudo-dual-Doppler analysis of a rear-inflow jet and deep convergence zone within a supercell. *Mon. Wea. Rev.*, **129**, 2270–2289.

—, A. L. Pazmany, J. C. Galloway, and R. E. McIntosh, 1995: Studies of the substructure of severe convective storms using a mobile 3-mm-wavelength Doppler radar. *Bull. Amer. Meteor. Soc.*, **76**, 2155–2169.

—, S. G. Gaddy, D. C. Dowell, A. L. Pazmany, J. C. Galloway, R. E. McIntosh, and H. Stein, 1997: Doppler radar observations of substorm-scale vortices in a supercell. *Mon. Wea. Rev.*, **125**, 1046–1059.

—, —, and —, 2003a: Mobile Doppler radar observations of a tornado in a supercell near Bassett, Nebraska, on 5 June 1999. Part I: Tornadogenesis. *Mon. Wea. Rev.*, **131**, 2954–2967.

—, —, —, W.-C. Lee, and M. Bell, 2003b: Mobile Doppler radar observations of a tornado in

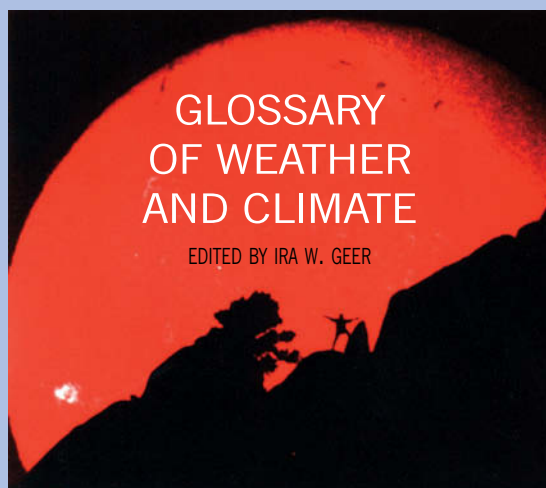
- a supercell near Bassett, Nebraska, on 5 June 1999. Part II: Tornado-vortex structure. *Mon. Wea. Rev.*, **131**, 2968–2984.
- , —, and —, 2004: The vertical structure of a tornado near Happy, Texas, on 5 May 2002: High-resolution, mobile, W-band, Doppler radar observations. *Mon. Wea. Rev.*, **132**, 2325–2337.
- , M. M. French, R. L. Tanamachi, S. Frasier, K. Hardwick, F. Junyent, and A. L. Pazmany, 2007a: Close-range observations of tornadoes in supercells made with a dual-polarization, X-band, mobile Doppler radar. *Mon. Wea. Rev.*, **135**, 1522–1543.
- , C. C. Weiss, M. M. French, E. Holthaus, R. L. Tanamachi, S. Frasier, and A. L. Pazmany, 2007b: The structure of tornadoes near Attica, Kansas, on 12 May 2004: High-resolution, mobile, Doppler radar observations. *Mon. Wea. Rev.*, **135**, 475–506.
- , M. M. French, I. PopStefanija, R. T. Bluth, and J. B. Knorr, 2010a: A mobile, phased-array Doppler radar for the study of severe convective storms. *Bull. Amer. Meteor. Soc.*, **91**, 579–600.
- , and Coauthors, 2010b: A summary of data collected during VORTEX-2 by MWR-05XP/TWOLF, UMass X-Pol, and the UMass W-band radar. Preprints, *25th Conf. on Severe Local Storms*, Denver, CO, Amer. Meteor. Soc., 5.4. [Available online at <http://ams.confex.com/ams/pdfpapers/176197.pdf>.]
- Brandes, E. A., 1978: Mesocyclone evolution and tornadogenesis: Some observations. *Mon. Wea. Rev.*, **106**, 995–1011.
- Brooks, H. E., and C. A. Doswell III, 2001: Normalized damage from major tornadoes in the United States: 1890–1999. *Wea. Forecasting*, **16**, 168–176.
- , —, and J. Cooper, 1994: On the environments of tornadic and nontornadic mesocyclones. *Wea. Forecasting*, **9**, 606–618.
- , M. T. Carr, and J. E. Ruthford, 1996: Preliminary analysis of soundings from VORTEX-95. *Proc. 18th Conf. on Severe Local Storms*. San Francisco, CA, Amer. Meteor. Soc., 133–136.
- Bryan, G. H., and M. D. Parker, 2010: Observations of a squall line and its near environment using high-frequency rawinsonde launches during VORTEX2. *Mon. Wea. Rev.*, **138**, 4076–4097.
- Burgess, D. W., R. A. Brown, L. R. Lemon, and C. R. Safford, 1977: Evolution of a tornadic thunderstorm. *Proc. 10th Conf. on Severe Local Storms*, Omaha, NE, Amer. Meteor. Soc., 84–89.
- , M. A. Magsig, J. Wurman, D. C. Dowell, and Y. Richardson, 2002: Radar observations of the 3 May 1999 Oklahoma City tornado. *Wea. Forecasting*, **17**, 456–471.
- Byko, Z., P. Markowski, Y. Richardson, J. Wurman, and E. Adelman, 2009: Descending reflectivity cores in supercell thunderstorms observed by mobile radars and in a high-resolution numerical simulation. *Wea. Forecasting*, **24**, 155–186.
- Clark, A. J., and Coauthors, 2011: Probabilistic precipitation forecast skill as a function of ensemble size and spatial scale in a convection-allowing ensemble. *Mon. Wea. Rev.*, **139**, 1410–1418.
- Davies-Jones, R. P., 1982a: A new look at the vorticity equation with application to tornadogenesis. *Proc. 12th Conf. on Severe Local Storms*, San Antonio, TX, Amer. Meteor. Soc., 249–252.
- , 1982b: Observational and theoretical aspect of tornadogenesis. *Intense Atmospheric Vortices*, L. Bengtsson and J. Lighthill, Eds., Springer-Verlag, 175–189.
- , 1984: Streamwise vorticity: The origin of updraft rotation in supercell storms. *J. Atmos. Sci.*, **41**, 2991–3006.
- , and H. E. Brooks, 1993: Mesocyclogenesis from a theoretical perspective. *The Tornado: Its Structure, Dynamics, Prediction, and Hazards, Geophys. Monogr.*, Vol. 79, Amer. Geophys. Union, 105–114.
- , R. J. Trapp, and H. B. Bluestein, 2001: Tornadoes and tornadic storms. *Severe Convective Storms, Meteor. Monogr.*, No. 50, Amer. Meteor. Soc., 167–222.
- Doswell, C. A., and D. W. Burgess, 1993: Tornadoes and tornadic storms: A review of conceptual models. *The Tornado: Its Structure, Dynamics, Prediction, and Hazards, Geophys. Monogr.*, Vol. 79, Amer. Geophys. Union, 161–172.
- Dowell, D. C., and H. B. Bluestein, 1997: The Arcadia, Oklahoma, storm of 17 May 1981: Analysis of a supercell during tornadogenesis. *Mon. Wea. Rev.*, **125**, 2562–2582.
- , and —, 2002a: The 8 June 1995 McLean, Texas, storm. Part I: Observations of cyclic tornadogenesis. *Mon. Wea. Rev.*, **130**, 2626–2648.
- , and —, 2002b: The 8 June 1995 McLean, Texas, storm. Part II: Cyclic tornado formation, maintenance, and dissipation. *Mon. Wea. Rev.*, **130**, 2649–2670.
- , Y. P. Richardson, and J. M. Wurman, 2002: Observations of the formation of low-level rotation: The 5 June 2001 Sumner County, Kansas tornado. Preprints, *21st Conf. on Severe Local Storms*, San Antonio, TX, Amer. Meteor. Soc., 12.3. [Available online at <http://ams.confex.com/ams/pdfpapers/47335.pdf>.]
- , F. Zhang, L. J. Wicker, C. Snyder, and N. A. Crook, 2004: Wind and temperature retrievals in the 17 May

- 1981 Arcadia, Oklahoma, supercell: Ensemble Kalman filter experiments. *Mon. Wea. Rev.*, **132**, 1982–2005.
- , C. R. Alexander, J. M. Wurman, and L. J. Wicker, 2005: Centrifuging of hydrometeors and debris in tornadoes: Radar-reflectivity patterns and wind-measurement errors. *Mon. Wea. Rev.*, **133**, 1501–1524.
- Fierro, A. O., M. S. Gilmore, E. R. Mansell, L. J. Wicker, J. M. Straka, and E. N. Rasmussen, 2006: Electrification and lightning in an idealized boundary-crossing supercell simulation of 2 June 1995. *Mon. Wea. Rev.*, **134**, 3149–3172.
- Finley, C. A., and B. D. Lee, 2004: High-resolution mobile mesonet observations of RFD surges in the June 9 Bassett, Nebraska, supercell during Project ANSWERS 2003. Preprints, *22nd Conf. on Severe Local Storms*, Hyannis, MA, Amer. Meteor. Soc., P11.3. [Available online at <http://ams.confex.com/ams/pdfpapers/82005.pdf>]
- , and —, 2008: Mobile mesonet observations of an intense RFD and multiple RFD gust fronts in the May 23 Quinter, Kansas tornadic supercell during TWISTEX 2008. Preprints, *24th Conf. on Severe Local Storms*, Savannah, GA, Amer. Meteor. Soc., P3.18. [Available online at <http://ams.confex.com/ams/pdfpapers/142133.pdf>]
- Fouts, L., 2003, Flow visualization and fluid-structure interaction of tornado-like vortices. M.S. thesis, Dept. of Mechanical Engineering, Texas Tech University, 131 pp.
- Frame, J. W., and P. M. Markowski, 2010: Numerical simulations of radiative cooling beneath the anvils of supercell thunderstorms. *Mon. Wea. Rev.*, **138**, 3024–3047.
- , —, Y. Richardson, J. Straka, and J. Wurman, 2009: Polarimetric and dual-Doppler radar observations of the Lipscomb County, Texas, supercell thunderstorm on 23 May 2002. *Mon. Wea. Rev.*, **137**, 544–561.
- Fujita, T. T., 1975: New evidence from the April 3–4, 1974 tornadoes. *Proc. Ninth Conf. on Severe Local Storms*, Norman, OK, Amer. Meteor. Soc., 248–255.
- Gilmore, M. S., and L. J. Wicker, 2002: Influences of the local environment on supercell cloud-to-ground lightning, radar characteristics, and severe weather on 2 June 1995. *Mon. Wea. Rev.*, **130**, 2349–2372.
- Grzych, M. L., B. D. Lee, and C. A. Finley, 2007: Thermodynamic analysis of supercell rear-flank downdrafts from Project ANSWERS. *Mon. Wea. Rev.*, **135**, 240–246.
- Hastings, R. M., and Y. P. Richardson, 2010: Storm mergers. Part 1: Preliminary numerical investigations of merger events. Preprints, *25th Conf. on Severe Local Storms*, Denver, CO, Amer. Meteor. Soc., 7A.5. [Available online at <http://ams.confex.com/ams/pdfpapers/176048.pdf>]
- Hirth, B. D., J. L. Schroeder, and C. C. Weiss, 2008: Surface analysis of the rear-flank downdraft outflow in two tornadic supercells. *Mon. Wea. Rev.*, **136**, 2344–2363.
- Houston, A. L., and R. B. Wilhelmson, 2011: The dependence of storm longevity on the pattern of deep convection initiation in a low-shear environment. *Mon. Wea. Rev.*, **139**, 3125–3138.
- Kennedy, A. D., J. M. Straka, and E. N. Rasmussen, 2007a: A statistical study of the association of DRCs with supercells and tornadoes. *Wea. Forecasting*, **22**, 1192–1199.
- , —, and —, 2007b: A visual observation of the 6 June 2005 descending reflectivity core. *Electron. J. Severe Storms Meteor.*, **2**, 1–12.
- Kosiba, K., and J. Wurman, 2010: The three-dimensional axisymmetric wind field structure of the Spencer, South Dakota, 1998 tornado. *J. Atmos. Sci.*, **67**, 3074–3083.
- , R. J. Trapp, and J. Wurman, 2008: An analysis of the axisymmetric three-dimensional low level wind field in a tornado using mobile radar observations. *Geophys. Res. Lett.*, **35**, L05805, doi:10.1029/2007GL031851.
- Kramar, M. R., H. B. Bluestein, A. L. Pazmany, and J. D. Tuttle, 2005: The “Owl Horn” radar signature in developing southern plains supercells. *Mon. Wea. Rev.*, **133**, 2608–2634.
- Lee, B. D., B. F. Jewett, and R. B. Wilhelmson, 2000: Supercell differentiation and organization for the 19 April 1996 Illinois tornado outbreak. Preprints, *20th Conf. on Severe Local Storms*, Orlando, FL, Amer. Meteor. Soc., P6.13. [Available online at https://ams.confex.com/ams/Sept2000/techprogram/paper_16459.htm]
- , C. A. Finley, and T. M. Samaras, 2011: Surface analysis near and within the Tipton, Kansas, tornado on 29 May 2008. *Mon. Wea. Rev.*, **139**, 370–386.
- Lee, J., T. Samaras, and C. Young, 2004: Pressure measurements at the ground in an F-4 tornado. Preprints, *22nd Conf. on Severe Local Storms*, Hyannis, MA, Amer. Meteor. Soc., 15.3. [Available online at <http://ams.confex.com/ams/pdfpapers/81700.pdf>]
- Lee, W.-C., and J. Wurman, 2005: The diagnosed structure of the Mulhall tornado. *J. Atmos. Sci.*, **62**, 2373–2393.
- Lemon, L. R., 1976: The flanking line, a severe thunderstorm intensification source. *J. Atmos. Sci.*, **33**, 686–694.
- , and C. A. Doswell, 1979: Severe thunderstorm evolution and mesocyclone structure as related to tornadogenesis. *Mon. Wea. Rev.*, **107**, 1184–1197.

- Lilly, D. K., 1982: The development and maintenance of rotation in convective storms. *Intense Atmospheric Vortices*, L. Bengtsson and J. Lighthill, Eds., Springer-Verlag, 149–160.
- Ludlam, F. H., 1963: Severe local storms: A review. *Severe Local Storms, Meteor. Monogr.*, No. 27, Amer. Meteor. Soc., 1–30.
- Maddox, R. A., L. R. Hoxit, and C. F. Chappell, 1980: A study of tornadic thunderstorm interactions with thermal boundaries. *Mon. Wea. Rev.*, **108**, 322–348.
- Magsig, M. A., and D. C. Dowell, 2004: Evolution of the hook echo and low-level rotation in the 17 May 2000 Brady, NE supercell. Preprints, *22nd Conf. on Severe Local Storms*, Hyannis, MA, Amer. Meteor. Soc., 14.3. [Available online at <http://ams.confex.com/ams/pdfpapers/81978.pdf>.]
- Markowski, P. M., and Y. P. Richardson, 2009: Tornado genesis: Our current understanding, forecasting considerations, and questions to guide future research. *Atmos. Res.*, **93**, 3–10.
- , E. N. Rasmussen, and J. M. Straka, 1998a: The occurrence of tornadoes in supercells interacting with boundaries during VORTEX-95. *Wea. Forecasting*, **13**, 852–859.
- , —, —, and D. C. Dowell, 1998b: Observations of low-level baroclinity generated by anvil shadows. *Mon. Wea. Rev.*, **126**, 2942–2958.
- , J. M. Straka, E. N. Rasmussen, and D. O. Blanchard, 1998c: Variability of storm-relative helicity during VORTEX. *Mon. Wea. Rev.*, **126**, 2959–2971.
- , —, and —, 2002: Direct surface thermodynamic observations within the rear-flank downdrafts of nontornadic and tornadic supercells. *Mon. Wea. Rev.*, **130**, 1692–1721.
- , —, and —, 2003: Tornadogenesis resulting from the transport of circulation by a downdraft. *J. Atmos. Sci.*, **60**, 795–823.
- , E. Rasmussen, J. Straka, R. Davies-Jones, Y. Richardson, and R. J. Trapp, 2008: Vortex lines within low-level mesocyclones obtained from pseudo-dual-Doppler radar observations. *Mon. Wea. Rev.*, **136**, 3513–3535.
- , M. Majcen, Y. P. Richardson, J. Marquis, and J. Wurman, 2011: Characteristics of the wind field in three nontornadic low-level mesocyclones observed by the Doppler on Wheels radars. *Electron. J. Severe Storms Meteor.*, **6**, 1–48.
- , and Coauthors, 2012a: The pretornadic phase of the Goshen County, Wyoming, supercell of 5 June 2009 intercepted by VORTEX2. Part I: Evolution of kinematic and surface thermodynamic fields. *Mon. Wea. Rev.*, in press.
- , and Coauthors, 2012b: The pretornadic phase of the Goshen County, Wyoming, supercell of 5 June 2009 intercepted by VORTEX2. Part II: Intensification of low-level rotation. *Mon. Wea. Rev.*, in press.
- Marquis, J. N., Y. P. Richardson, J. M. Wurman, and P. M. Markowski, 2008: Single- and dual-Doppler analysis of a tornadic vortex and surrounding storm scale flow in the Crowell, Texas, supercell of 30 April 2000. *Mon. Wea. Rev.*, **136**, 5017–5043.
- , —, P. Markowski, D. Dowell, and J. Wurman, 2012: Tornado maintenance investigated with high-resolution dual-Doppler and EnKF analysis. *Mon. Wea. Rev.*, **140**, 3–27.
- Marshall, T. P., 2002: Tornado damage survey at Moore, Oklahoma. *Wea. Forecasting*, **17**, 582–598.
- , 2004: The enhanced Fujita (EF) scale. Preprints, *22nd Conf. on Severe Local Storms*, Hyannis, MA, Amer. Meteor. Soc., 3B.2. [Available online at <http://ams.confex.com/ams/pdfpapers/81090.pdf>.]
- Marwitz, J., and D. W. Burgess, 1994: The observed inflow structure of a thunderstorm with a mesocyclone. *Mon. Wea. Rev.*, **122**, 393–396.
- McDonald, J. R., 2001: T. Theodore Fujita: His contribution to tornado knowledge through damage documentation and the Fujita scale. *Bull. Amer. Meteor. Soc.*, **82**, 63–72.
- Palmer, R., and Coauthors, 2009: Weather radar education at the University of Oklahoma—An integrated interdisciplinary approach. *Bull. Amer. Meteor. Soc.*, **90**, 1277–1282.
- Rasmussen, E. N., and J. M. Straka, 2007: Evolution of angular momentum in the 2 June 1995, Dimmitt, Texas, tornado. *J. Atmos. Sci.*, **64**, 1365–1378.
- , —, R. P. Davies-Jones, C. A. Doswell, F. H. Carr, M. D. Eilts, and D. R. MacGorman, 1994: Verification of the Origins of Rotation in Tornadoes Experiment: VORTEX. *Bull. Amer. Meteor. Soc.*, **75**, 995–1006.
- , S. Richardson, J. M. Straka, P. M. Markowski, and D. O. Blanchard, 2000: The association of significant tornadoes with a baroclinic boundary on 2 June 1995. *Mon. Wea. Rev.*, **128**, 174–191.
- , J. M. Straka, M. S. Gilmore, and R. P. Davies-Jones, 2006: A preliminary survey of rear-flank descending reflectivity cores in supercell storms. *Wea. Forecasting*, **21**, 923–938.
- Richardson, Y. P., K. K. Droegemeier, and R. P. Davies-Jones, 2007: The influence of horizontal environmental variability on numerically simulated convective storms. Part I: Variations in vertical shear. *Mon. Wea. Rev.*, **135**, 3429–3455.
- Rotunno, R., 1981: On the evolution of thunderstorm rotation. *Mon. Wea. Rev.*, **109**, 577–586.

- , and J. B. Klemp, 1985: On the rotation and propagation of simulated supercell thunderstorms. *J. Atmos. Sci.*, **42**, 271–292.
- Rust, W. D., D. W. Burgess, R. A. Maddox, L. C. Showell, T. C. Marshall, and D. K. Lauritsen, 1990: Testing a mobile version of a Cross-Chain LORAN Atmospheric (M-CLASS) sounding system. *Bull. Amer. Meteor. Soc.*, **71**, 173–180.
- Selvam, R. P., and P. C. Millett, 2003: Computer modeling of the tornado forces on buildings. *J. Wind Eng. Struct.*, **6**, 209–220.
- Sengupta, A., F. L. Haan, P. P. Sarkar, and V. Balaramudu, 2008: Transient loads on buildings in microburst and tornado winds. *J. Wind Eng. Ind. Aerodyn.*, **96**, 2173–2187.
- Shabbott, C. J., and P. M. Markowski, 2006: Surface in situ observations within the outflow of forward-flank downdrafts of supercell thunderstorms. *Mon. Wea. Rev.*, **134**, 1422–1441.
- Stensrud, D. J., J. Gao, T. M. Smith, K. Manross, J. Brogden, and V. Lakshmanan, 2010: A realtime weather-adaptive 3DVAR analysis system with automatic storm positioning and on-demand capability. Preprints, *25th Conf. on Severe Local Storms*, Denver, CO, Amer. Meteor. Soc., 8B.1. [Available online at https://ams.confex.com/ams/25SLS/techprogram/paper_175886.htm.]
- Straka, J. M., E. N. Rasmussen, and S. E. Fredrickson, 1996: A mobile mesonet for fine-scale meteorological observations. *J. Atmos. Oceanic Technol.*, **13**, 921–936.
- , —, R. P. Davies-Jones, and P. M. Markowski, 2007: An observational and idealized numerical examination of low-level counter-rotating vortices toward the rear flank of supercells. *Electron. J. Severe Storms Meteor.*, **2**, 1–22.
- Tanamachi, R. L., H. B. Bluestein, W. C. Lee, M. Bell, and A. L. Pazmany, 2007: Ground-based velocity track display (GBVTD) analysis of W-band Doppler radar data in a tornado near Stockton, Kansas, on 15 May 1999. *Mon. Wea. Rev.*, **135**, 783–800.
- Trapp, R. J., 1999: Observations of nontornadic low-level mesocyclones and attendant tornadogenesis failure during VORTEX. *Mon. Wea. Rev.*, **127**, 1693–1705.
- , G. J. Stumpf, and K. L. Manross, 2005: A reassessment of the percentage of tornadic mesocyclones. *Wea. Forecasting*, **20**, 680–687.
- Verbout, S. M., H. E. Brookes, L. M. Leslie, and D. M. Schultz, 2006: Evolution of the U.S. tornado database: 1954–2003. *Wea. Forecasting*, **21**, 86–93.
- Wakimoto, R. M., and N. T. Atkins, 1996: Observations on the origins of rotation: The Newcastle tornado during VORTEX 94. *Mon. Wea. Rev.*, **124**, 384–407.
- , and C. Liu, 1998: The Garden City, Kansas, storm during VORTEX 95. Part II: The wall cloud and tornado. *Mon. Wea. Rev.*, **126**, 393–408.
- , and H. Cai, 2000: Analysis of a nontornadic storm during VORTEX 95. *Mon. Wea. Rev.*, **128**, 565–592.
- , C. Liu, and H. Cai, 1998: The Garden City, Kansas, storm during VORTEX 95. Part I: Overview of the storm life cycle and mesocyclogenesis. *Mon. Wea. Rev.*, **126**, 372–392.
- , N. T. Atkins, and J. Wurman, 2011: The LaGrange tornado during VORTEX2. Part I: Photogrammetric analysis of the tornado combined with single-Doppler radar data. *Mon. Wea. Rev.*, **139**, 2233–2258.
- Walko, R. L., 1993: Tornado spin-up beneath a convective cell: Required basic structure of the near-field boundary layer winds. *The Tornado: Its Structure, Dynamics, Prediction, and Hazards, Geophys. Monogr.*, Vol. 79, Amer. Geophys. Union, 89–95.
- Weckwerth, T. M., J. W. Wilson, and R. M. Wakimoto, 1996: Thermodynamic variability within the convective boundary layer due to horizontal convective rolls. *Mon. Wea. Rev.*, **124**, 769–784.
- Weiss, C. C., and J. L. Schroeder, 2008: StickNet: A new portable, rapidly deployable surface observation system. *Bull. Amer. Meteor. Soc.*, **89**, 1502–1503.
- , —, J. Guynes, P. S. Skinner, and J. Beck, 2009: The TTUKa mobile Doppler radar: Coordinated radar and in situ measurements of supercell thunderstorms during Project VORTEX2. Preprints, *34th Conf. on Radar Meteorology*, Williamsburg, VA, Amer. Meteor. Soc., 11B.2. [Available online at <http://ams.confex.com/ams/pdfpapers/155425.pdf>.]
- Wicker, L. J., and R. B. Wilhelmson, 1995: Simulation and analysis of tornado development and decay within a three-dimensional supercell thunderstorm. *J. Atmos. Sci.*, **52**, 2675–2703.
- Winn, W. P., S. J. Hunyady, and G. D. Aulich, 1999: Pressure at the ground in a large tornado. *J. Geophys. Res.*, **104 (D18)**, 22 067–22 082.
- Wurman, J., 1998: Preliminary results from the ROTATE-98 tornado experiment. *Proc. 19th Conf. on Severe Local Storms*, Minneapolis, MN, Amer. Meteor. Soc., 120–123.
- , 2001: The DOW mobile multiple Doppler network. Preprints, *30th Int. Conf. on Radar Meteorology*, Munich, Germany, Amer. Meteor. Soc., P3.3. [Available online at <http://ams.confex.com/ams/pdfpapers/21572.pdf>.]
- , 2002: The multiple vortex structure of a tornado. *Wea. Forecasting*, **17**, 473–505.
- , 2003: Multiple-Doppler observations of tornadoes and tornadogenesis during the ROTATE-2003

- project. Preprints, *31st Conf. on Radar Meteorology*, Seattle, WA, Amer. Meteor. Soc., P4A.1. [Available online at https://ams.confex.com/ams/32BC31R5C/techprogram/paper_63886.htm.]
- , 2008: Preliminary results and report of the ROTATE-2008 radar/in-situ/mobile mesonet experiment. Preprints, *24th Conf. on Severe Local Storms*, Savannah, GA, Amer. Meteor. Soc., 5.4. [Available online at https://ams.confex.com/ams/24SLS/techprogram/paper_142200.htm.]
- , and S. Gill, 2000: Fine-scale radar observations of the Dimmitt, Texas, tornado. *Mon. Wea. Rev.*, **128**, 2135–2164.
- , and T. Samaras, 2004: Comparison of in-situ pressure and DOW Doppler winds in a tornado and RHI vertical slices through 4 tornadoes during 1996–2004. Preprints, *22nd Conf. on Severe Local Storms*, Hyannis, MA, Amer. Meteor. Soc., 15.4 [Available online at <http://ams.confex.com/ams/pdfpapers/82352.pdf>.]
- , and C. R. Alexander, 2005: The 30 May 1998 Spencer, South Dakota, storm. Part II: Comparison of observed damage and radar-derived winds in the tornadoes. *Mon. Wea. Rev.*, **133**, 97–119.
- , J. Straka, and E. Rasmussen, 1996a: Fine scale Doppler radar observation of tornadoes. *Science*, **272**, 1774–1777.
- , —, and —, 1996b: Preliminary radar observations of the structure of tornadoes. *Proc. 18th Conf. on Severe Local Storms*, San Francisco, CA, Amer. Meteor. Soc., 17–22.
- , —, —, M. Randall, and A. Zahrai, 1997: Design and deployment of a portable, pencil-beam, pulsed, 3-cm Doppler radar. *J. Atmos. Oceanic Technol.*, **14**, 1502–1512.
- , C. Alexander, P. Robinson, and Y. Richardson, 2007a: Low-level winds in tornadoes and potential catastrophic tornado impacts in urban areas. *Bull. Amer. Meteor. Soc.*, **88**, 31–46.
- , Y. Richardson, C. Alexander, S. Weygandt, and P. F. Zhang, 2007b: Dual Doppler analysis of winds and vorticity budget terms near a tornado. *Mon. Wea. Rev.*, **135**, 2392–2405.
- , —, —, —, and —, 2007c: Dual-Doppler and single-Doppler analysis of a tornadic storm undergoing mergers and repeated tornadogenesis. *Mon. Wea. Rev.*, **135**, 736–758.
- , P. Robinson, W. Lee, C. R. Alexander, and K. A. Kosiba, 2008: Rapid-scan mobile radar 3D GBVTD and traditional analysis of tornadogenesis. Preprints, *24th Conf. on Severe Local Storms*, Savannah, GA, Amer. Meteor. Soc., P13.6. [Available online at <http://ams.confex.com/ams/pdfpapers/142176.pdf>.]
- , K. A. Kosiba, P. Markowski, Y. Richardson, D. Dowell, and P. Robinson, 2010: Finescale and dual-Doppler analysis of tornado intensification, maintenance, and dissipation in the Orleans, Nebraska, tornadic supercell. *Mon. Wea. Rev.*, **138**, 4439–4455.
- Xue, M., K. K. Droegemeier, and V. Wong, 2000: The Advanced Regional Prediction System (ARPS)—A multiscale nonhydrostatic atmospheric simulation and prediction tool. Part I: Model dynamics and verification. *Meteor. Atmos. Phys.*, **75**, 161–193.
- Ziegler, C. L., E. N. Rasmussen, T. R. Shepherd, A. I. Watson, and J. M. Straka, 2001: The evolution of low-level rotation in the 29 May 1994 Newcastle–Graham, Texas, storm complex during VORTEX. *Mon. Wea. Rev.*, **129**, 1339–1368.



Educators, students, and weather enthusiasts! A glossary of over 3000 terms on weather and climate designed specifically for a general audience! Produced under the Project ATMOSPHERE initiative, the development of The Glossary of Weather and Climate was inspired by increasing contemporary interest in the atmosphere and global change. The objective of the glossary is to provide a readily understandable, up-to-date reference for terms that are frequently used in discussions or descriptions of meteorological and climatological phenomena. In addition, the glossary includes definitions of related oceanic and hydrologic terms.

©1996 American Meteorological Society. Available in both hardcover and softcover, B&W, 272 pages, \$26.95 list/\$21.00 member (softcover); \$34.95 (hardcover) plus shipping and handling. Order online at www.ametsoc.org/amsbookstore. Please send prepaid orders to Order Department, American Meteorological Society, 45 Beacon St., Boston, MA 02108-3693.